http://pubs.acs.org/journal/acsodf

Review

Progress in Niobium Oxide-Containing Coatings for Biomedical Applications: A Critical Review

Mir Saman Safavi, F. C. Walsh, Livia Visai,* and Jafar Khalil-Allafi*

Cite This: *ACS Omega* 2022, 7, 9088−9107

Read Online

ACCESS | Metrics & More | Article Recommendations

ABSTRACT: Typically, pure niobium oxide coatings are deposited on metallic substrates, such as commercially pure Ti, Ti6Al4 V alloys, stainless steels, niobium, TiNb alloy, and Mg alloys using techniques such as sputter deposition, sol−gel deposition, anodizing, and wet plasma electrolytic oxidation. The relative advantages and limitations of these coating techniques are considered, with particular emphasis on biomedical applications. The properties of a wide range of pure and modified niobium oxide coatings are illustrated, including their thickness, morphology, microstructure, elemental composition, phase composition, surface roughness and hardness. The corrosion resistance, tribological characteristics and cell viability/proliferation of the coatings are illustrated using data from electrochemical, wear resistance and biological cell culture measurements. Critical R&D needs for the development of improved future niobium oxide coatings, in the laboratory and in practice, are highlighted.

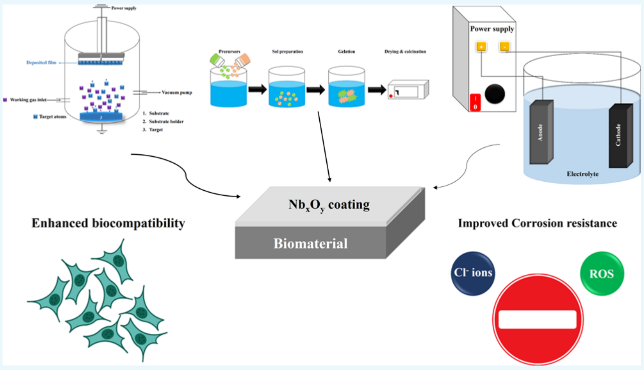

1. INTRODUCTION

Aging, illness, and accidents provide threats to human health. It is essential to seek appropriate materials and devices to aid repair or replacement of damaged body parts over extended periods.[1] According to a definition presented by American National Institute of Health, a biomaterial is "a synthetic or natural material or combination of the materials excluding drugs, which is deployed to partially or entirely replace any tissue/organ or maintain or enhance the life quality of the individuals." This definition excludes gypsum, waxes, finishing materials, etc.[2,3] The biomaterials should encourage favorable biological responses in the host tissue.[4] Depending on the type of constituent material, biomaterials can be broadly categorized as follows: (i) metallic, e.g., Ti and Ti-based alloys, Mg alloys, Co−Cr, stainless steel, NiTi; (ii) ceramic, e.g., calcium phosphates (CaP); (iii) polymer, e.g., polyurethane (PU); (iv) composite, e.g., CaP-PU; and (v) natural, e.g., skin.[5−14] It is important to appreciate the contributions made by biomaterials to modern medicine. They are used in a variety of clinical applications, including orthopedic, cardiovascular, facial, and dentistry treatments. The total market for bioimplants in 2020 is about 89 million USD, forecasted to grow with a compound annual growth rate (CAGR) of 6.5% during the time period of 2020−2026. Orthopedic implants hold the largest fraction of the global implant market. Over 22 million orthopedic surgeries take place annually worldwide, which is expected to reach about 28 million in 2022.[15−18]

Metallic materials are by far the most commonly employed synthetic bulk implants since they took advantage of high mechano-corrosion properties together with acceptable biological performance. The appropriate strength of these materials offers the opportunity to exploit them as load-bearing implants in dentistry and orthopedics.[19−25] The first scientific reports on the use of metals as synthetic implantable material traced back to 1895. For over 100 years, the development progress of metal implants has not been stopped so that the focus on controlling the overall properties of these implants to attain better performance has grown rapidly in recent years,[26] but several problems limit the successful long-term *in vivo* use of metallic implants:

- The presence of a harsh environment in the human body, wear between joints, and stress load cycles that may be repeated millions of times in a lifetime crucially challenge the implantation process. While corrosion of orthopedic implants may be caused by the presence of corrosive species, such as Cl^- ions, the low pH associated with the presence of F^- ions around dental

Received: January 21, 2022
Accepted: March 1, 2022
Published: March 11, 2022

https://doi.org/10.1021/acsomega.2c00440

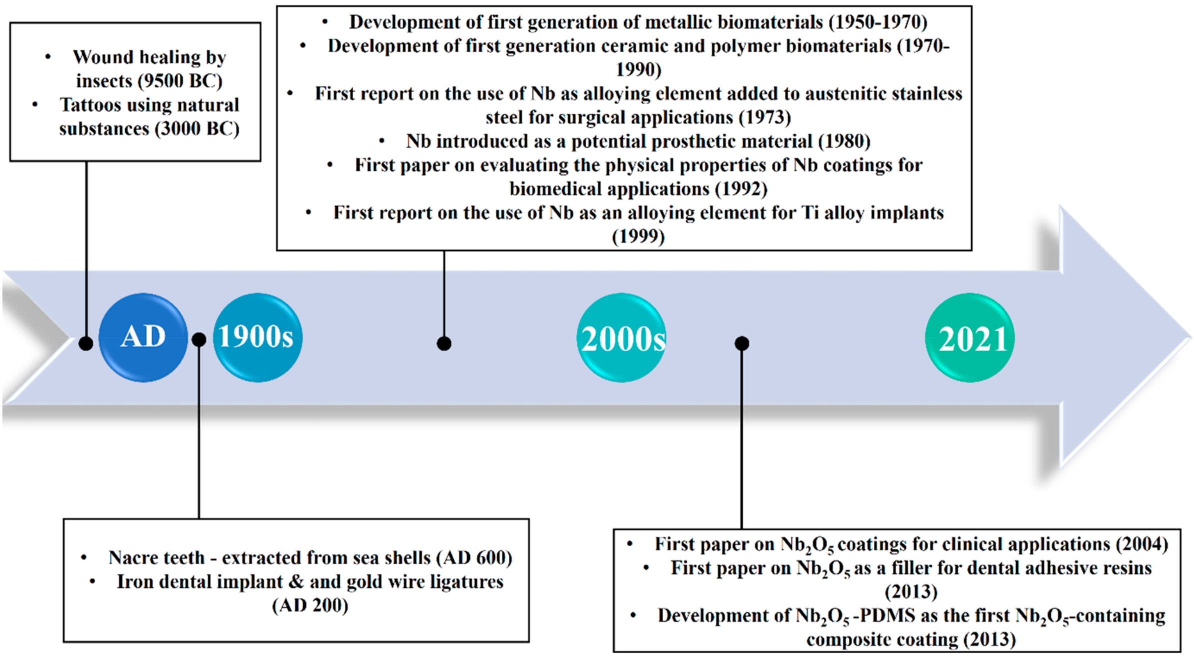

Figure 1. Timeline for the development of biomaterials, biomedical application of Nb, and biocompatible Nb_2O_5 coatings.[66−74]

implants can dominate during corrosion.[27] Although research in this field has placed a high premium on assessing the influence of the corrosive physiological medium on releasing the toxic ions, tribology plays a central role in realizing the concentration of the released ions especially in the knee, hip, joints, etc.[28] For instance, it is reported that 6.7 × 10^{13} to 2.5 × 10^{15} Co particles per year can be released from implanted Co−Cr material. When evaluating the Co level in the periprosthetic fluid of patients suffered from failed implants, it has been recognized that the Co level surpassed 22 mg/L, at least 4 times higher than in those without complaints. Furthermore, every step walk leads to the release of 10^6 debris nanoparticles from metalware.[29] NiTi, stainless steel, and Ti6Al4 V implants are the other materials that the ion release from their surface greatly threaten the implantation success and patient's health, by inducing allergic reactions.[30] It is important to adopt effective, empirical strategies to increase the corrosion resistance of biomaterials. This not only prolongs the service lifetime of the implant but also avoids inflammation.

- The mismatch between the elastic modulus of the synthetic implant material and natural bone, which can lead to stress shielding. While the elastic modulus of the natural bone is in the range of 10−40 GPa, Co−Cr alloys and stainless steels show an elastic modulus above 200 GPa. This can substantially decrease the bone density (osteopenia) since the implanted material with higher elastic modulus bears the applied loads.[31−33]
- Insufficient osseointegration, which refers to the inefficiency of the implanted material in enabling an appropriate platform for apatite to nucleate and grow at the implant/host tissue interface. When the material is implanted *in vivo*, the present proteins adsorb on the surface of the implant. Hence, the surface condition of the biomaterial plays a major role in osseointegration. Under *in vivo* conditions, different cells, such as osteoblasts, fibroblasts, and endothelials come into contact with the biomaterial for tissue remodeling. As a brief summary, the more the bioactive surface, the higher the integration between the implant and host tissue occurs. Among the common metallic biomaterials, stainless steels can suffer from a lack of bioactivity.[34−40]
- Bacterial infection: when the biomaterial is implanted *in vivo*, in particular for knee joints and dental applications, a competition between the present microorganisms and host cells starts to occupy the largest fraction of the surface of the biomaterial, so-called "race for the surface". If the microorganisms win this race, bacterial colonies can be formed over the surface, leading to the preprosthetic infection that can damage the local tissues. To avoid the mentioned challenge at an early stage of implantation, and to get higher implantation efficiency, it is necessary to adopt cost-effective, flexible, and feasible strategies.[41−46]

The surface of the implant is the place where the first interactions between implant and host cell/tissue occur. Surface-related features, encompassing topography, energy, and chemical composition, determine the protein adsorption, osseointegration quality, and implant fixation. It is possible to change the final characteristics of the bulk implant by modifying its surface so that the surface, i.e., the initial interaction site, offers quite different functions compared to the bulk implant.[47−53] To date, a variety of surface finishing techniques, including electrochemical deposition,[54] sol−gel,[55] sputter deposition,[56] spray deposition,[57] biomimetic deposition,[58] as well as coating materials, such as CaP,[59] TiO_2,[60] ZrO_2,[61] ZnO,[62] Nb_2O_5,[63] etc., have been proposed to induce favorable properties to the surface of the biomaterials. For instance, it is possible to induce bioactivity for superior osseointegration by the application of CaP family coatings or prevent bacterial inflammations through deposition of silver or zinc-containing layers. These strategies can open new windows to develop the new generation of implants that bypass the challenges faced by metal implants and can avoid putting an additional burden on the patient.[64] The nanostructured topography of the surface of the biomaterials brings forth promising perspectives since a vast majority of the biological interactions, such as osteoblast adhesion and biomineralization, occur on the nanoscale, and the nanometric surface roughness can appreciably affect the adhesion process.[65] Figure 1 illustrates a timeline for the development of biomaterials, biomedical application of Nb, and biocompatible Nb_2O_5 coatings.

The present review paper attempts to discuss the properties, application, and market of niobium and its oxides, putting emphasis on their biomedical properties and applications. The overall characteristics of the pure Nb_xO_y and Nb_xO_y-containing coatings deposited by various surface finishing techniques will also be treated in detail, putting stress on the importance of surface finishing with pure Nb_xO_y and Nb_xO_y-containing layers along with a relationship between the operating parameters and final properties of the resultant films.

2. IMPORTANT PROPERTIES OF NIOBIUM AND NIOBIUM OXIDE

Niobium (Nb) is a refractory metal, possessing high thermal stability, erosion-resistant properties, low vapor pressure, good chemical stability in a variety of hostile environments, excellent corrosion resistance, suitable tribomechanical properties, e.g., high wear resistance, excellent ductility at room temperature, favorable biocompatibility, and low thermal expansion. Nb falls under the category of transition metals, crystallizing in a body-centered cubic (BCC) crystal lattice.[75−79] Table 1 lists some of the physical properties of the Nb.

Table 1. Some of the Physical Properties of the Nb[80,81]

physical properties	amount
melting point	2447 °C
boiling point	4741 °C
density	8.57 g cm^{-3}
electrical resistivity	15.2 $\mu\Omega$ cm at 273 K
relative atomic mass	92.906

Regarding biological characteristics of Nb, it is a nontoxic and allergy-free metal, indicting acceptable biocompatibility and osteoconductivity.[82−84] As in the case of titanium (Ti), Nb is known as an "essential metal" since it enables significant chemical stability in the physiological medium. Therefore, Nb is considered as a potential metallic element in fabrication of synthetic implantable materials and devices for soft and hard tissues.[85] Thanks to its promising properties, the main focus of research has been to realize the *in vitro* and *in vivo* performance of Nb and in particular Nb-containing alloys. Results of a comparative work on the biological performance of Nb, Ti, and stainless steel, as three important and useful synthetic implant materials, showed that there are much more mitochondrial activity and cell proliferation on Nb compared to the others. The highest rate of the *in vivo* osseointegration of tested implants is also registered for Nb.[86,87] To fabricate bulk synthetic implants, it is encouraged to alloy the Nb with other biocompatible materials, such as Ti, rather than using it in its pure form. When alloyed with Ti, Nb can stabilize the β phase, which contributes to decreasing the elastic modulus of Ti, thereby diminishing the risk of the "stress shielding". Moreover, the positive role of this element in improving corrosion and biological features of the composite implants should not be neglected.[72,88,89]

Besides technical aspects, cost and availability during materials selection for the fabrication of a synthetic implant can be critical.[90] Brazil has the largest Nb reserves, equivalent to approximately 98.53% of total Nb in the world. Nb ore reserves exceed 212 billion tonnes in Brazil, which makes this country the biggest producer of Nb, about 96% of world production. Brazil is followed by Canada and Australia, which contain 1.01% and 0.46% of world's Nb ores reserves, respectively.[91−93] Interestingly, Europe is the main consumer of Nb, where 30% of total Nb is consumed. Worldwide, Nb is supplied in various forms, including niobium pentoxide (Nb_2O_5), niobium carbide (NbC), metal niobium, ferro-niobium alloy (FeNb), and lithium niobate ($LiNbO_3$). Furthermore, it is possible to purchase niobium pentachloride ($NbCl_5$) only from Russia. FeNb dominates the global production of Nb-containing materials. FeNb is used for fabrication of high strength steels, occupying about 89% of Nb world production. It is to be noted that the largest application of Nb is corresponded to structure steels, more than 34% of total Nb market. Overall, the total Nb market value is about 1389 USD in 2019, which is anticipated to stand at 1748 USD by the end of 2027.[94]

The tremendous osteoconductivity, biocompatibility, and corrosion performance of Nb are dominated by the oxide layer formed over its surface. The corrosion properties of the formed oxide layer determine the overall corrosion resistance of the Nb in acidic or neutral environments. Among various oxides, Nb_2O_5 is the most common type of niobium oxide and can be spontaneously generated over the surface when Nb is exposed to an oxygen-containing environment. It is tightly adherent to the Nb and can fully cover its surface.[86,95−99] Nb_2O_5 illustrates high resistance against both corrosion and wear, excellent thermodynamic, thermal, and chemical stabilities, high reflective index, low density, outstanding mechanical strength, and fracture toughness, nontoxicity, hypoallergenic, great biological characteristics, enabling cellular attachment, growth, spreading, proliferation, metabolic activity, collagen synthesis, seriously influencing endothelial cell responses, alkaline phosphatase activity (ALP), and supporting HAp formation in the various physiological media due to the small lattice mismatch (1.1%) between the oxide and mineral HAp phase.[73,100−110] Due to the above properties, Nb_2O_5 coatings show significant potential for applications in a variety of industrial applications, such as electrochromic devices, optical windows, solar cells, sensing devices, catalysts, supercapacitors, and biomedical.[111,112] Although the initial interests in Nb_2O_5 and its polymorphs, e.g., NbO_6, are traced back to the 1940s, the potential benefits and applications of Nb_2O_5 have not been fully exploited so far. In the early years, the main industrial applications of this transition metal were as sensors and catalysts, in which Nb_2O_5 was used in the bulk or film form.[113,114] Recently, the biomedical applications of Nb_2O_5 in bulk and coating form have drastically increased owing to their exceptional biological features. Synthetic orthopedic implants, biosensors, and radiopacifying agent coupled with Portland cement in dentistry and filler for dental adhesive resin are important medical applications of Nb_2O_5.[72,112,115,116]

3. PURE NB_XO_Y COATINGS

Background. Typically, pure niobium oxide coatings are deposited over a variety of metallic substrates, including commercially pure Ti, Ti6Al4 V alloys, stainless steels (particularly AISI 316L grade), Nb, TiNb alloy, and Mg alloys using techniques such as sputter deposition, sol−gel deposition, anodizing, and wet plasma electrolytic oxidation (PEO).[117−121]

Magnetron-sputtered pure Nb_2O_5 coatings can be obtained using a Nb metallic target in either pure oxygen[117,122] or mixed oxygen + argon atmospheres.[123,124] To deposit sol−gel derived Nb_2O_5 coatings, three types of sols can be prepared using various precursors with specific molar ratios as below: (i) butanol, acetylacetone, and niobium alkoxide;[121,125] (ii) niobium ethoxide, *iso*-propanol, acetylacetone, and polyethylene glycol (PEG);[126] and (iii) niobium butoxide, triethanolamine, ethanol, and PEG.[127]

The anodizing of Nb-containing substrates can be carried out from three types of electrolyte: (i) NaF or Na_2HPO_4-containing HF(aq);[118] (ii) a mixture of $Ca(H_2PO_4)_2$, $Ca(OOCCH_3)_2$, and $C_{10}H_{14}N_2Na_2O_8$;[88] and (iii) a mixture of $C_2H_6O_2$ and NH_4F.[128]

PEO coating of Nb anode material can be carried out from phosphoric acid and hydrogen peroxide-containing and calcium acetate monohydrate electrolytes. It is also possible to employ a bath composed of a mixture of phosphoric acid and calcium acetate monohydrate.[120] Table 2 provides the advantages, limitations, and schematic illustration of common techniques employed for achieving pure niobium oxide coatings.

The published literature on the evaluation of final characteristics of pure Nb_xO_y coatings has emphasized the influence of the coatings on the overall performance of the underlying implants, drawing relationships between the role of operating parameters and properties of the resultant coating and providing an insight into the biological performance of metal oxide coatings, such as Nb_2O_5, Ta_2O_5, and TiO_2.[105,124,138] The following text will provide a systematic overview of the properties of pure Nb_xO_y coatings.

Morphology and Topography. The surface morphology and topography of the Nb_xO_y deposits are highly dependent on the type of the employed coating technique, applied operating factors, and post-treatments. Among the various niobium oxides, Nb_2O_5 coatings have attracted increasing attention. Regardless of the coating method, four different types of surface morphologies: conelike,[118] nodular,[138] granular,[91] and spheroidal[120] have been observed for Nb_2O_5 coatings.

Overall, the surface of the pure coatings produced via the radio frequency (RF) magnetron sputtering and reactive sputtering methods are homogeneous, tightly adherent to the substrate, and without visible defects, such as cracks and discontinuities. The constituent particles are uniformly arranged over the surface of the coating.[91,117,139,140] The surface topography of the films confirmed the formation of a densely packed surface without surface-related defects.[91,117,139,140] It has been claimed that the application of magnetron sputtering can ensure formation of a dense and uniform coating.[124] The insertion of nitrogen gas during RF magnetron sputtering can lead to the formation of niobium-oxynitride coating, in which a higher degree of the crystallinity is seen in deposits from a high gas flow rate. This can also give rise to surface roughness. While amorphous coatings are grown in an equiaxial fashion, crystalline deposits tend to be columnar.[138]

Published literature on the surface morphology of the sol−gel derived films is very contradictory. While some reports demonstrated the formation of the coatings containing a network of pores with different diameters from nanometer to micrometers by sol−gel dip coating,[105,127] one study confirmed the formation of a crack-free surface with a low porosity content through sol−gel spin coating even after calcination at 500 °C.[126] The aim behind the application of the calcination is to eliminate solvent and residual organics, convert oxides, and achieve a crystalline deposit.[126] However, the evaporated solvent can lead to pore generation in the so-called "evaporation induced self-assembly process", which can significantly decrease the density of the obtained film. It should

Table 2. Advantages, Limitations, and Schematic Illustration of the Common Techniques Used to Apply Pure Niobium Oxide Coatings[129−137]

Deposition technique	Advantage	Limitations	Schematic
Sputter deposition	Uniform and dense coatings; homogenous film, tightly adherent to the substrate.	Low deposition rate; expensive; line of sight technique.	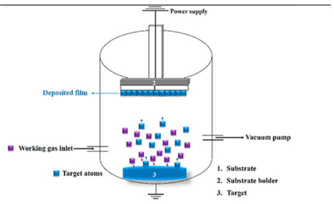
Sol-gel	High purity; uniform thickness; ability to coat substrates having a complex geometry; moderate cost; enhanced mechano-corrosion protection properties.	Pilot-scale production; porous microstructure, need for post-treatments; possibility of crack formation.	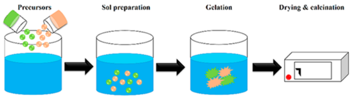
Anodizing	Adherent coatings; high corrosion resistance; low-cost; simplicity.	Decreases some materials properties, e.g., thermal conductivity; long duration of process, low hardness, heating of anodes; so-called "burning", due to high local current density edge effects.	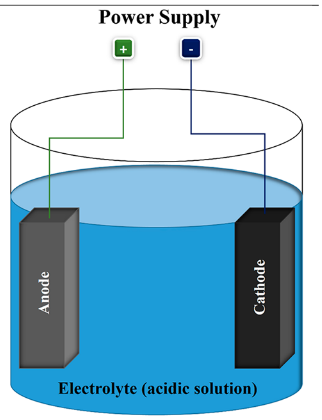
Plasma electrolytic oxidation	Eco-friendly method for production of ceramic coatings; short duration of process; excellent tribocorrosion properties.	Porous microstructure; requires high cell voltage; complex, pulsed and a.c. waveforms may be necessary.	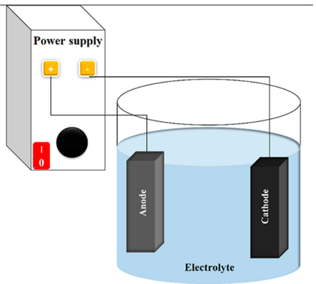

be noted that the pores remain at the top surface of the film and may have little effect on the mechano-corrosion properties of the coatings.[105,127,141] Moreover, the sol−gel derived Nb_xO_y films are susceptible to blistering originated from the difference between the coefficient of thermal expansion (CTE) of the underlying metallic implant and ceramic top layer.[126,142] The constituent particles of the sol−gel derived films include both spherical[125] and wavy[126] morphologies. The formation of some aggregated particles over the surface of the films have also been reported.[126] Although the deposited oxide coating increases the surface roughness of the underlying substrate, the degree of increment greatly depends on the calcination temperature. Eisenbrath et al.[121] have indicated that the surface roughness of the Nb_2O_5 coatings increased from 7 to 40 nm when the calcination temperature was raised from 450 to 700 °C. The nanoporous nature of the sol−gel derived coatings is the reason why the deposited film enhances the surface roughness of the substrate. The higher the surface roughness, the superior bioactivity and biocompatibility are obtained,[105,143] which will be comprehensively discussed in the following text.

The operating parameters involved in the anodizing process, e.g., time, cell voltage applied, and acid concentration, noticeably affect the surface morphology of the deposited films. The prolonged anodization time from 20 to 90 min results in a change in the morphology of the coating from amorphous to the self-assembled crystalline one, consisting of microcones. Such a microstructure can be emerged when the oxygen ions diffuse through the newly formed oxide layer and interact with the present Nb ions that are present over the underlying substrate. The presence of salts in the acidic electrolyte determines the morphology and porosity content of the formed microstructure.[118,144,145] Furthermore, at longer anodizing times, a higher rate of oxide growth is seen.[146] It is reported that the deposition of Nb_2O_5 layer over the Nb foil changes its morphology through formation of some small pores. The content, distribution, and size of the pores crucially depends on the applied potential. While the surface of oxide films fabricated at the potential of 200 V contains 2 μm-sized pores with quite uniform dispersion, those deposited under 250 V show heterogeneous surfaces with three-time larger pores. The applied potential not only varies the surface characteristics but also changes the thickness and surface roughness, where a thicker layer with higher surface roughness can be obtained when a higher potential is applied.[88] The type and concentration of acidic electrolyte have significant influence on the surface properties. The lower the HF(aq) concentration leads to the higher oxide layer growth. The as-reached F^- ions to the surface of Nb metal interact with the interstitial Nb ions to form Nb_2O_5.[146]

Contradictory results have been reported on the surface morphology of Nb_2O_5 coatings obtained by PEO deposition. While Pereira et al.[120] showed the formation of the compact surface with spheroidal particles after PEO in phosphoric acid solution, Lokeshkumar et al.[147] demonstrated that the deposited layer was porous, consisting of interconnected open pores. It is stated that the chemical composition of the used solution and operating parameters determine the homogeneity of the Nb_2O_5 deposit. For instance, the film produced from $Na_3SiO_4 \cdot 12H_2O$ + KOH electrolyte under a final cell voltage of 80 V had a heterogeneous surface containing microcracks, while that deposited from $Na_3PO_4 \cdot 9H_2O$ + KOH at a final cell voltage of 75 V produced a uniform surface morphology. In general, the use of a silicate bath leads to thicker deposits.[147] It is also possible to couple the PEO route with other electrochemical deposition technique, such as electrophoretic deposition (EPD), to incorporate desired second phase to the growing oxide layer[147] and apply two-step PEO with various electrolyte composition.[120] For example, biocompatible hydroxyapatite (HAp) particles can be incorporated to the PEO-fabricated Nb_2O_5 film via EPD. The included particles markedly affect the surface properties of the oxide layer with closing the pores and diminishing their size.[147] Table 3 summarizes the thickness and surface roughness of the Nb_xO_y coatings deposited via different methods on a variety of substrates.

Table 3. Thickness and Surface Roughness of the Nb_xO_y Coatings Deposited via Different Methods on Various Substrates[a]

coating method	substrate type	thickness/nm	surface roughness (R_a)/nm	refs
magnetron sputtering	Ti6Al4 V	210	2.4 ± 0.5	117
RF magnetron sputtering	cp Ti	121.63		148
magnetron sputtering	Ti6Al4 V	210	2.4 ± 0.5	139
magnetron sputtering	Ti6Al4 V	180	16.5	122
magnetron sputtering	Ti6Al4 V	210		140
RF magnetron sputtering	316L stainless steel	688.5−825.9	2.05−3.41	138
reactive magnetron sputtering	Ti6Al4 V	300−450		91
reactive and nonreactive magnetron sputtering	AISI 316LVM steel		18.5	124
DC magnetron sputtering	316L stainless steel	300	2.94	123
sol−gel	cp Ti	100	7−40	121
sol−gel	316L stainless steel	$2-3 \times 10^3$	18.6	126
sol−gel	β-type Ti alloy	160	4−50	125
sol−gel	AZ31 Mg alloy	2×10^3	26.75	105
anodizing	Nb	$2-13 \times 10^3$	130−900	88

[a] A change in the deposition technique or processing parameters can significantly alter the surface characteristics.

Microstructure. The published results regarding the atomic arrangement of the sputter deposited Nb_2O_5 coatings show differences. While an enormous majority of the reports indicated that the magnetron sputtered films are amorphous,[117,122,139,149] there is a study confirming the generation of a crystalline Nb_2O_5 coating via magnetron sputtering at 60 °C.[148] Deposition at low temperature and a lack of substrate heating during the deposition process are the main reasons explaining the generation of an amorphous Nb_2O_5 layer.[117,122,139] The postheat treatment of the crystalline Nb_2O_5 coatings at 700 °C for 60 min leads to the emergence of new Nb_2O_5 and βNb_2O_5 peaks as well as changing the height and width of existing peaks.[148] The oxygen/nitrogen gas flow ratio realizes the atomic arrangement of the sputtered niobium oxynitride film. The amorphous coating changes to the polycrystalline one when the oxygen content exceeds beyond a threshold. In such a condition, film growth is dependent on the oxygen and niobium reaction even if nitrogen flows into the vacuum chamber. The presence of nitrogen led to a niobium oxynitride coating without changing the crystal lattice.[138,150]

Sol−gel derived coatings can be either amorphous or crystalline depending on the temperature of the must be carefully established. While Pradhan et al.[119] showed that the films calcined at 450 °C are amorphous and crystalline transformation occurred above 500 °C, Amaravathy et al.[105] approved the deposition of the sol−gel derived crystalline Nb_2O_5 layer through calcination at 380 °C. The films calcined at about 500 °C are composed of a hybrid amorphous + crystalline lattice. A rise in calcination temperature not only leads to the appearance of some new Nb_2O_5 peaks but also changes the unit cell geometry of the lattice. For instance, a change in unit cell geometry from hexagonal to orthorhombic is obtained at the calcination temperature above 575 °C.[119] Table 4 outlines the crystallite size of the sol−gel derived Nb_2O_5 films as a function of calcination temperature. The crystallite size of the coatings is measured using the Scherrer equation as follows:[151−153]

Table 4. Crystallite Size of the Sol−Gel Derived Nb_2O_5 Films as a Function of Calcination Temperature

type of sol−gel film deposition	calcination temperature/°C	atomic arrangement/unit cell	crystallite size/nm	refs
not mentioned	500	mixture of amorphous + crystalline	23 ± 4	119
	550	crystalline/hexagonal	37 ± 6	
	575	crystalline/hexagonal	43 ± 3	
	650	crystalline/orthorhombic	74 ± 3	
dip-coating	500	crystalline/hexagonal	30−40	127
dip-coating	380	crystalline/monoclinic	48	105
spin-coating	500	crystalline/hexagonal	41.49	126
spin-coating	550	not mentioned	24	155
	600		38	
	650		39	
	700		58	

$$D = \frac{k\lambda}{\beta \cos \theta} \tag{1}$$

where k, λ, β, and θ are the Scherrer constant, wavelength of X-ray, fwhm, and Bragg angle, respectively. The Scherrer constant depends on the crystallite shape. For instance, it is taken to be 0.89 for spherical crystallites.[154]

As seen, all of the sol−gel derived coatings are nanostructured, which provide a larger surface area to interact with the cells improving the cell adhesion and adsorption of proteins.[105]

The phase structure of the Nb_2O_5 produced via anodization of Nb substrate is only composed of peaks assigned to the orthorhombic Nb_2O_5.[118]

PEO-coated Nb_2O_5 are crystalline and can be present in both hexagonal and orthorhombic unit cell geometry.[120,147] Although the composition of the acidic electrolyte used in the PEO process has no influence on the emerged phases, it can only alter the height and width of the emerged peaks.[147]

Tribomechanical Behavior. The implanted material should benefit from appropriate tribomechanical properties since it endures normal and shear forces as well as undergoing friction during the service time. This issue is particularly highlighted for dental and orthopedic implants. Thus, the method and composition of the coating should be controlled in such a way that meet the required tribomechanical properties. Also, the bonding strength and durability of the coating should be taken into consideration since the film may detach as a result of the forces endured.[156−158] Meanwhile, there should be a balance between the elastic modulus of the implant material and natural bone, especially for orthopedic implants. A big mismatch can result in “stress-shielding”, which eventually causes a failure in implantation. For instance, the elastic modulus values of the stainless steel and cortical bone are 180 and 17 GPa, respectively. Such a mismatch can lead to stress-shielding. Surface modification of the implants is needed to satisfy mechanical and chemical requirements.[159,160] Nanoindentation, nanoscratching, pull-off tensile testing, wear testing, and corrosion studies can be employed to analyze the tribomechanical characteristics of biocoatings.[161−164]

The application of the Nb_2O_5 coating by the sputter deposition route can greatly raise the nanohardness and elastic modulus of the metallic implants, in particular the Ti-based ones. It is reported that the nanohardness and elastic modulus of the Ti6Al4 V implant increases from ≈5.5 to ≈8.6 GPa and from 112 to 142 GPa, respectively.[117,122,139,140] The sputter deposited Nb_2O_5 films possess desirable tribological performance as there are no scratches detected on the surface of the coatings after a steel wool test under a load of 0.5 N.[117,122,139] Kalisz et al.[140] have demonstrated that the nanohardness of the coatings negligibly decreases, about 5%, after a corrosion test in a corrosive medium containing NaCl and KF. The surface morphology of the Nb_2O_5 coating after a tribocorrosion test, which provides a perspective on the synergistic action of corrosion and wear, in Ringer’s solution under the normal load of 5 N at rotating speed of 5 rpm that applies to a bone pin indicating the formation of some pits together with a sign of an adhesive wear track. In general, it is claimed that the Nb_2O_5 layer offers tremendous wear resistance; however, it could be degraded when it underwent wear in a corrosive, *in vivo* environment.[124] An SEM micrograph of a Nb_2O_5 coating after tribocorrosion testing is shown in Figure 2. The sign of adhesive wear is observable for Nb_2O_5 coating after the tribocorrosion assay.

The results of an *in vivo* assay can enable a more realistic view of the mechanical performance of the coatings. The *in vivo* removal of torque is a suitable characterization method to reveal whether the osseointegration is sufficiently firm. The sputter deposited Nb_2O_5 layer shows an acceptable torque value. The value was enhanced with time, confirming the generation of a favorable implant/bone bonding, which can promote bone growth and facilitate mechanical interlocking between the coating and underlying implant.[148]

The application of Nb_2O_5 coating via a sol−gel route gives rise to the hardness of the metallic implant. Moreover, the elastic modulus of the layer is much lower than that of underlying metallic substrate due to its porous microstructure, decreasing the risk of stress-shielding effect. The sol−gel derived ceramic layer possesses high bonding strength, qualifying its use in orthopedic applications.[126]

The adhesion strength between the PEO-fabricated Nb_2O_5 coating and Nb substrate is reported to be sufficient for

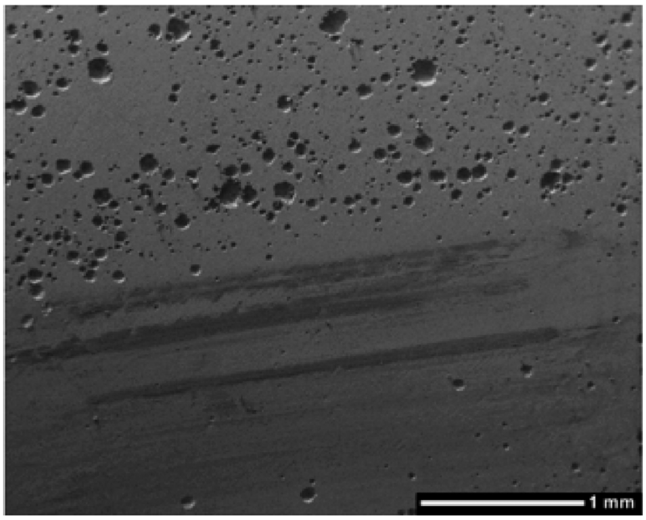

Figure 2. SEM micrograph of Nb_2O_5 coating after tribocorrosion testing.[124] Reprinted with permission from ref 124. Copyright 2021 by the authors.

biomedical applications, irrespective of the composition of the used electrolyte.[120] Table 5 summarizes the reported mechanical properties of Nb_xO_y biocoatings.

Information on tribomechanical properties of the Nb_xO_y biocoatings is scarce in the open literature. For future works, establishing the mechanisms involved in a change in the tribomechanical properties with the application of Nb_xO_y coating, identifying relationships between the processing parameters and tribomechanical performance of the resultant deposit, studying all of the tribomechanical aspects, encompassing hardness, elastic modulus, interfacial strength, and tribocorrosion response of the coatings, should be addressed in detail.

Corrosion Performance. In general, the corrosion resistance of the metallic implants, including Ti6Al4 V and 316L stainless steel, outstandingly promotes when they are protected by sputter deposited Nb_2O_5 coatings. However, the factors governing such an enhancement in the corrosion behavior have not been clearly considered in the literature.[117,122,139,140] In the case of an uncoated metallic implant, e.g., Ti6Al4 V, a passive layer can be formed over its surface when it is immersed in the corrosive medium. Since the Ti has a negative reversible potential, it is susceptible to oxidation upon exposing to aqueous electrolytes. The passive layer contributes to the corrosion resistance through providing an initial barrier against the present corrosive species. It is to be emphasized that the protective capability of the layer directly depends on the pH of the medium so that the layer cannot resist against aggressive anions.[165,166] There are practical works that provide a comparative insight into the corrosion protection performance of the ceramic coatings, e.g., Nb_2O_5, NbN, and TiO_2, in the biological media. For instance, Ramirez et al.[149] have reported that sputter deposited Nb_2O_5 provided stronger corrosion protection than that of NbN produced by the same technique. On the other hand, Orozco-Hernández et al.[124] have revealed the better corrosion inhibition of TiO_2 compared to Nb_2O_5 without correlating the results with their morphological and microstructural characteristics. Unlike TiO_2 films, the sputter deposited Nb_2O_5 ones are prone to fall into pitting corrosion.

The sol−gel produced Nb_2O_5 coatings improve the corrosion resistance of the underlying metallic substrates since they can act as a potential barrier against corrosive species.[105,125−127] Unlike bare substrate, a passive film forms over the coated one when it is immersed into the corrosive electrolyte.[105] Although the breakdown potential obtained from the potentiodynamic polarization assay is dependent on the oxygen evolution at substrate/coating interface, by which the corrosive species reach to the substrate via cracks and/or pores passage, the potential values of bare and coated-substrate reveal that the porous nature of the sol−gel derived films did not adversely affect their corrosion resistance. The simulated body fluid (SBF)-soaked Nb_2O_5 coatings show much higher corrosion resistance than that of as-deposited Nb_2O_5 due to the fact that the immersion in SBF leads to an apatite layer, which provides an extra blocking barrier and prevents the dissolution of the metal ions.[126,127,167] It is well established that the volume of the evolved hydrogen when an implant is immersed in SBF alters the biocompatibility of the surrounding cells. Thus, the corrosion resistant material, which produces lower hydrogen volume in SBF, is more biocompatible. There are much lower hydrogen bubbles emerged over the surface of the Nb_2O_5-coated AZ31 Mg alloy than bare alloy, contributing to its better biological characteristics.[105] The results of a comparative study of the corrosion performance of the several sol−gel derived metal oxide coatings on Ti implants revealed that the Nb_2O_5 coating has the lowest corrosion resistance without addressing the parameters lead to difference in resistance of the coatings.[125]

Anodized Nb substrates show better corrosion behavior compared with the bare Nb.[88,168] The improvement degree deeply depends on the cell voltage during anodizing. Canepa et al.[88] have reported that the corrosion resistance of the anodized Nb linearly increases with the increase in cell voltage from 0 to 200 V, followed by a slight drop with a further rise up to 250 V. While the increased thickness and better morphological properties of the oxide layer leads to enhanced corrosion resistance, a higher porosity content degrades the resistance of the samples produced at 250 V. Results of a comparative work revealed that the formed oxide layer during the anodization of Ta and Nb possesses superior corrosion protection than that of Ti While Nb_2O_5 coatings deposited by

Table 5. Reported Mechanical Properties of Nb_xO_y Biocoatings

coating type	deposition method	characterization method	hardness	elastic modulus/GPa	refs
Nb_2O_5	sputter deposition	nanoindentation	8.64 GPa	142	117
Nb_2O_5	sputter deposition	nanoindentation	8.64 GPa		139
Nb_2O_5	sputter deposition	nanoindentation	5.58 ± 0.3 GPa		122
Nb_2O_5	sputter deposition	nanoindentation	8.64 GPa (before corrosion)		140
			8.16 GPa (after corrosion in NaCl and KF-containing media)		
Nb_2O_5	sol−gel	Vickers microhardness	444 ± 3.2 HV		126

https://doi.org/10.1021/acsomega.2c00440
ACS Omega 2022, 7, 9088−9107

Table 6. Corrosion Parameters of the Nb_xO_y Biocoatings Deposited by Various Methods[a]

coating type	deposition method	test medium	highest E_{corr}/mV	lowest j_{corr}/μA cm^{-2}	highest R_p/kΩ	highest R_{ct}/kΩ	ref
Nb_2O_5	sputter deposition	0.5 M/L NaCl, 2 g/L KF; pH 2 at room temperature	−401	0.24			117
Nb_2O_5	sputter deposition	0.5 M/L NaCl, 2 g/L KF; pH 2 at room temperature	−401	0.24			139
Nb_2O_5	sputter deposition	0.5 mol/L NaCl, 2 g/L KF; pH 2 at room temperature	−251	0.09			122
Nb_2O_5	sputter deposition	0.5 mol/L NaCl, 2 g/L KF; pH 2 at room temperature	−401	0.24			140
Nb_2O_5	sputter deposition	8.9 g/L NaCl; pH 7.4 at room temperature		0.12	3200		149
Nb_2O_5	sputter deposition	Ringer's solution, at 37 ± 0.2 °C	−170	22.1		52.8	124
Nb_2O_5	sol−gel	SBF, at room temperature	−202			141.41	126
Nb_2O_5	Sol−gel	0.9% NaCl, pH 7.4 at 37 °C		83	4820		125
Nb_2O_5	sol−gel	SBF, pH 7.4	−1586 ± 49	53.2 ± 4			105
Nb_2O_5	anodizing	Ringer's solution, at 37 °C	−200		32400	29	88
Nb_2O_5	PEO	SBF, pH 7.4	−472.97	0.0218			147

[a] E_{corr}, j_{corr}, and R_p obtained from potentiodynamic polarization are corrosion potential, corrosion current density, and polarization resistance, respectively. R_{ct} values are charge transfer resistance obtained from electrochemical impedance spectroscopy (EIS).

PEO on the Nb substrate promote its corrosion behavior, the enhancement is not marked due to the high porosity of the film. In addition, the thickness and phase composition of the deposit govern the corrosion protection efficiency. The PEO process that performed in silicate-based solution has superior corrosion resistance to that produced from phosphate-based electrolyte may be due to the lower porosity content.[147,169] Table 6 lists the corrosion parameters of the Nb_xO_y biocoatings deposited by various methods.

Biological Characteristics. The biological characteristics of the pure Nb_xO_y coatings, including cell viability, adhesion, proliferation, differentiation, and growth along with the ability of the oxide coatings to provide a favorable substrate for nucleation and growth of stoichiometric HAp upon immersion in the SBF, and antibacterial activity, are of the important aspects that have been addressed in the literature.[119,120,149,155]

Overall, the published results on the influence of sputter deposited Nb_xO_y coatings on the biological characteristics of underlying implants show pronounced differences. While a vast majority of the results confirmed the improvement of the coating characteristics is related to the type of the underlying substrate. Unlike Nb_2O_5-coated 316L SS,[123] the application of Nb_2O_5 layer over the Ti6Al4 V degrades the cell adhesion and proliferation. The reason addressing such a different behavior is assigned to the higher hydrophobicity of the Nb_2O_5 layer than that of Ti6Al4 V.[149]

The enhanced performance of the coated-implants is attributed to the synergistic role of higher hydrophilic nature, surface roughness, and more polarized structure of the Nb_xO_y. The level of improvement in the biological properties is a function of surface topography, wettability, and atomic order, which can be controlled by operating parameters involved in the sputtering technique. For example, the Nb_2O_5 coatings sputter deposited under a higher N_2/O_2 gas ratio offer superior human fibroblast cell adhesion due to their amorphous atomic order.[138]

As an important factor realizing the biocompatibility of a synthetic implanted material, besides cell compatibility, the material should not lead to a harmful inflammation when it comes in contact with living cells and tissues. Corrosion and abrasion occurrence in the physiological medium can result in the inflammatory due to the released toxic ions from the surface of the material, thereby failing the implantation.[170−172] IL-10 and IL-17 are of anti-inflammatory cytokines, which play a key role in impeding inflammatory, e.g., chronic inflammatory and autoimmune pathologies. Moreover, TNF-α deals with inflammation prevention and osteoblast activation.[173,174] The Nb_2O_5-coated metallic substrates induce higher anti-inflammatory cytokines, revealing their excellent capability in diminishing the toxicity.[91,123]

The antibacterial activity of the metallic implant is highly improved with protecting its surface by sputter deposited NbO_xN_y coating. The antibacterial activity of the coatings against *S. aureus* is promoted when the atomic order is changed from amorphous to crystalline with tuning the N_2/O_2 gas ratio.[138]

The sol−gel derived Nb_2O_5 deposits benefit from the appropriate biological properties; however, the processing parameters in particular calcination time and temperature markedly alter the properties. Besides, the immersion time can also govern the features of the formed apatite layer.[74,119,126,127] The *in vitro* bioactivity assay by immersing the sample into the SBF solution containing an analogous ionic composition to human blood plasma is a preliminary route to realize whether the sample is bioactive. If the incubated material supports the formation of apatite, it is bioactive. The more compact the apatite layer is formed and chemical composition is closer to that of stoichiometric HAp, i.e., Ca/P = 1.67, the better bioactivity is obtained. The results of SBF soaking assay give a reliable view of *in vivo* bone bonding, where the sample that cannot stimulate the apatite formation is not qualified for further *in vivo* assays.[175−178] Pradhan et al.[119] have observed that the platelike apatite crystals are generated over the surface of the sol−gel derived Nb_2O_5 coating calcined at 525 °C after immersion in SBF for 30 days, while the calcination at lower and higher temperatures, e.g., 450 and 650 °C, as well as immersion for 1−7 days do not stimulate apatite formation. The difference in the bioactivity of the coatings has been ascribed to their various atomic arrangement and unit cell geometry, where the hexagonal-Nb_2O_5 coating possesses bioactivity but amorphous and orthorhombic-Nb_2O_5 ones do not. Oxygen depletion and oxide vacancies may seriously affect

Table 7. Biological Properties of Pure Nb_xO_y Coatings[a]

coating type	deposition method	type of cultured cell	assay type	% highest cell viability/%	highest reported absorbance	apatite generation ability	refs
NbO_xN_y	sputter deposition	healthy human lung fibroblast cell line (MRC5)	MTT	125 ± 5			138
Nb_2O_5	sputter deposition	cells derived from a human cementoblastoma	MTT		0.49		149
Nb_2O_5	sol−gel	mouse fibroblast cell line L-929	MTT	105 ± 45			119
Nb_2O_5	sol−gel	MC3T3-E1 osteoblast cell	direct contact	102 ± 10			121
Nb_2O_5	sol−gel	HPMEC* endothelialcells	triplicate assay		1.2 ± 0.1		185
Nb_2O_5	PEO	fibroblast cell line L-929	MTT	83			147

[a] HPMEC: Primary human pulmonary microvascular endothelial cells.

the bioactivity of oxide-containing coatings. It is essential to perform in-depth studies to address their role in the bioactivity of Nb_xO_y coatings.

The implant/cell interaction is greatly affected by the surface characteristics of the implant, such as chemical composition, surface roughness, surface energy, and surface wettability.[179−181] During the initial stage of implantation, when the surrounding cells are connected to the implant, the material adsorbs the existing proteins in the body fluid, such as vitronectin and fibronectin, to provide a desirable platform for cell adhesion and osseointegration. At higher values of hydrophilicity, i.e., at lower contact angles, the number of adsorbed proteins over the surface of the implant is increased, leading to superior cell adhesion and improved implant/cell interaction. The higher surface roughness results in a higher surface wettability.[182−184] The sol−gel Nb_2O_5-coated implants have more hydrophilic surface than bare ones irrespective of the chemical composition of the implant and the medium used for contact angle measurement.[105,126]

Depending on the operating factors involved in the sol−gel technique, which alter the surface roughness and phase structure of the Nb_2O_5 deposit, the deposit can variously affect the cell viability.[119,121,155] For instance, while hexagonal-Nb_2O_5 coating showed a slight decrease in cell viability after 30 days of incubation, orthorhombic-Nb_2O_5 did not influence the number of living cells. The various unit cell geometry is obtained due to the difference in the calcination temperature. Although Nb_2O_5 coatings show no toxicity to the cells, in-depth studies are required to address how the crystalline structure changes the biological behavior of the coatings.[119] The different surface roughness originating from various calcination times and temperatures determines the cell viability, where the highest cell number is attained for the Nb_2O_5 film with the smoothest surface. It is emphasized that the influence of surface roughness on the cell adherence rate can be neglected at longer incubation times. Whether the surface roughness alters the osteoblast adhesion greatly depends on the atomic arrangement of the coating. While the surface roughness has no influence on the cell spreading in the crystalline coating, the amorphous deposit with low surface roughness facilitates the spreading. Moreover, the increased surface roughness of the Nb_2O_5 film, e.g., at a surface roughness of 15 and 40 nm, promotes the collagen-I synthesis, where there is no dense collagen-I layer formed over the film with a roughness of 7 nm.[121,155]

Vascular stent grafts are largely employed in aortic aneurysms and coronary bypasses. Development of synthetic vascular grafts, which possess both high performance and durability are of prime significance as there is still a serious fail in stenting, about 10−25% out of total cases. To address this issue and develop a hybrid ceramic coated-metallic stent, Chai et al.[185] have made a comparative insight into the performance of cp Ti that coated by various biocompatible ceramic coatings. They have reported both TiO_2 and Nb_2O_5, coatings deposited by the sol−gel technique show favorable homocompatibility, while SiO_2 is less homocompatibile. They have also inferred that the Nb_2O_5-coated Ti exhibits the highest endothelial cell proliferation after various days of incubation.

As mentioned earlier, the bioactivity of the implant can be examined via immersion in some standard media, containing various salts and proteins that simulate *in vivo* conditions, including SBF, simulated salvia, phosphate buffer saline (PBS), Dulbecco's Modified Eagle's Medium (DMEM), etc.[118,186,187] The results of *in vitro* bioactivity assay carried out in human saliva medium, which is different with simulated saliva due to encompassing more than 43 proteins and enzymes, such as statherin and mucins, etc., indicated that the microcone shaped Nb_2O_5 formed during the anodization of Nb foil in the electrolyte composed of 2.5 wt % HF(aq) and 100 mg of NaF can support mineral formation. The phase structure of the minerals is consisted of Hap.[118,188,189] Elemental analysis showed a higher phosphorus content than calcium in the structure of the film.[118] This indicates the presence of an intermediate amorphous phase, covering the underlying HAp crystals.[190]

In general, the PEO fabricated Nb_2O_5 coatings are more hydrophilic than the underlying Nb substrate. However, the chemical composition of the electrolyte bath can slightly alter the wettability.[120,147] For instance, the coatings produced from silicate-based solutions are more hydrophilic than those deposited from phosphate-based electrolytes. Evaluating the biocompatibility of the PEO produced Nb_2O_5 coatings with a variety of assays, such as 3-(4,5-dimethylthiazol-2-yl)-2,5-diphenyl tetrazolium bromide (MTT), apoptosis test, direct contact assay, confirms that they are nontoxic and the cultured cells over their surface can stay alive and grow.[147] Table 7 outlines the biological properties of pure Nb_xO_y coatings.

4. NB_XO_Y-CONTAINING COATINGS

Background. Irrespective of the applied surface finish technique, the deposited pure Nb_xO_y coatings may face several drawbacks. One practical way to address these drawbacks and induce new beneficial properties to the pure Nb_xO_y coatings is incorporating elements or compounds into the pure coating. The concept of "composite coating" is a potential approach that leads to fruitful results in this case. The included reinforcing agent can be either organic or inorganic chemicals. PEG,[148] CuO,[122] graphene,[122] cerium (Ce),[191] zinc (Zn),[192] copper (Cu),[140] and erythromycin[43] are examples of reinforcing phases that have been successfully included to enhance the final properties of the pure Nb_xO_y coatings. There are also some studies that have exploited Nb_2O_5 as a secondary phase to develop more efficient biocoatings, which are encompassed in this section.[73,110] Apart from the well-established deposition techniques, e.g., sputter deposition and sol−gel, Nb_xO_y-containing layers can also be obtained through annealing the CaP-coated Nb-containing substrates[193] and/or air plasma spraying of Nb coatings.[194] The following text presents the characteristics of the Nb_xO_y-containing coatings based on the type of the added material(s).

Metallic Additives. Cu, Ce, and Zn are the metallic elements that have been incorporated into the Nb_2O_5 coatings to provide special properties and functions to them. The metallic element-reinforced Nb_2O_5 coatings can be deposited through sputter deposition and sol−gel routes.[117,140,191,192] In the former case, an extra target composed of the desired element is coupled with the Nb target, leading to the metallic element-reinforced Nb_2O_5 coating. The amount of the reinforcing phase in the resultant film can be controlled either via changing the operating parameters or the amount of element in the target.[117] To obtain sol−gel derived metallic element-reinforced Nb_2O_5 deposits, a sol corresponding to the additive composition is prepared, followed by adding the as-prepared sol to the Nb_2O_5 sol. The content of additives in the deposited film can be tailored by varying the concentration of the precursors in the sol.[191,192] For instance, the concentration of zinc nitrate hexahydrate in the sol governs the content of Zn in the sol−gel Zn−Nb_2O_5 composite deposits.[192]

Cu is an essential trace element, known as the most active biological active metal, playing a central role in catalyzing metabolic processes. It also contributes to the angiogenesis and bone formation. Excellent activity of the Cu, in particular Cu^{2+} cation as the most active form of Cu, against microorganisms along with negligible cytotoxicity makes it a propitious candidate for antibacterial applications.[195−197] Cu−Nb_2O_5 composite coatings are obtained using the magnetron sputtering technique. The addition of Cu to the Nb_2O_5 deposit markedly affects the surface-related characteristics, where a more smooth and homogeneous surface is obtained. The rounded particles formed in microstructure of the pure coatings disappear with the inclusion of Cu.[117,140] The surface roughness of the Nb_2O_5 decreases with incorporation of the Cu, followed by a slight increase in roughness with further increase in the content of Cu in the coating. However, the surface roughness of the composite layers is still much less than that of pure film.[117] Tribomechanical properties, including nanohardness, elastic modulus, and scratch resistance of the Nb_2O_5 films, degrade when the Cu is included in the film. A 10% and 26% decrease in nanohardness and elastic modulus is reported for Nb_2O_5-25 at % Cu composite coatings compared to Nb_2O_5 coating, respectively. The introduction of a noble metal to the ceramic coating promotes its corrosion resistance.[117] The more Cu that is included, the higher the corrosion protection obtained.[117,140] The postcorrosion surface morphology reveals that, unlike the pure Nb_2O_5 layer, there is no change in morphology of the composite films due to the slow generation of the passive layer over the composite film.[140] Unlike the Nb_2O_5 layer, the nanohardness of the composite coating did not change after corrosion assay. The diminished nanohardness of the pure film is attributed to the formation of the passive layer during the assay.[140,198,199] The contact angle of composite coating is slightly higher than that of pure layer, irrespective of the type of employed droplet.[117]

Recently, tremendous attention has been paid to Ce in biomedical applications due to its exponential corrosion resistance. In its oxide form, Ce gives rise to the biological responses of the cultured cells, such as proliferation and differentiation.[200,201] Katta et al.[191] have merely studied the influence of Ce content in the structure of sol−gel derived Ce-included Nb_2O_5 coating on final characteristics of the produced layer without addressing how embedded metallic additives can affect the properties of pure Nb_2O_5 coating. They have reported that an increase in Ce content from 1 to 2 wt % has no noticeable effect on the morphology and phase structure of the films. However, the higher Ce amount in the film leads to the enhanced thickness and surface roughness. On the other hand, the hydrophilicity and corrosion protection efficiency of the sol−gel layers enhance with a higher included Ce phase. The Ce-reinforced Nb_2O_5 coatings exhibit self-healing behavior within the anodic region of the potentiodynamic polarization curve. The formed cerium oxides and/or hydroxides can prevent corrosion progress through healing the present defects over the surface of the sol−gel film. The following reactions may occur within the anodic region:[202,203]

$$O_2^{\bullet -} + Ce^{4+} \rightarrow O_2 + Ce^{3+} \tag{2}$$

$$O_2^{\bullet -} + Ce^{3+} + 2H^+ \rightarrow H_2O_2 + Ce^{4+} \tag{3}$$

Regardless of the content of included Ce, Ce-included Nb_2O_5 films illustrate appropriate biocompatibility where osteoblast cells can attach and spread over the surface of the films due to the presence of porous and rough surfaces. Moreover, an increase in Ce content has constructive influence on the biocompatibility.[191]

Similar to Cu, Zn is an essential element, playing a major role in mineralization, metabolic functions, cell signaling, and immune system performance. High antibacterial performance of the Zn offers the prospect of using Zn as a strong antibacterial agent.[192,204] The present microcracks all over the microstructure of the sol−gel derived Nb_2O_5 films that are generated due to difference between the CTE of the top layer and biomaterial can be eliminated by addition of Zn to the pure coating. This can contribute to a higher hardness and corrosion resistance.[67,192] Furthermore, the increased Zn content not only changes the surface morphology but also raises the surface roughness. Unlike morphological characteristics, the phase composition of the films do not change with Zn inclusion. Compared to pure Nb_2O_5, Zn-reinforced ones illustrate higher *in vitro* bioactivity through facilitating the precipitation of higher amounts of mineral stoichiometric HAp. There is an inverse relation between the content of Zn in the Zn-incorporated Nb_2O_5 layer and the measured contact angle value. It is reported that there is an optimum content for Zn at the highest corrosion performance. In such an optimum condition, the highest compactness, crystallinity, and sufficient thickness are obtained. Simply put, increasing the Zn amount for any percent may degrade this property. The included Zn considerably improves the antibacterial activity of the pure Nb_2O_5 layer owing to the formation of ZnO in the structure of the layer.[192] The formed ZnO can inhibit bacteria adhesion and suppress their growth via enabling a desirable platform for generation of reactive oxygen species (ROS), e.g., O^{2-}, OH^-,

Table 8. Mechanical Properties of the Particle-Strengthened Nb_2O_5 Composite Layers

type of reinforcing phase	studied variable (amount)	deposition technique	characterization method	highest reported hardness	highest reported elastic modulus/GPa	refs
Cu	content of reinforcing phase; 17−25 at %	magnetron sputtering	nanoindentation	7.79 GPa	105	117
Cu	composite film containing constant content of 25 at %	magnetron sputtering	nanoindentation	7.79 GPa		140
Zn	molar ratios of Nb to Zn: ranging from 0.5:0 to 0.5:0.75	sol−gel	Vickers	363 HV		192
CuO	composite film containing constant content of CuO	magnetron sputtering	nanoindentation	7.19 GPa		122

H_2O_2, that severely harms bacteria.[205] The higher surface roughness and presence of functional active groups over the surface of Zn-reinforced Nb_2O_5 films facilitate the osteoblast cell adhesion and proliferation.[192]

Ceramic Additives. Recently, a rising interest has been seen in using CuO for biomedical applications owing to its excellent physicochemical properties and high antibacterial and antimicrobial performance against a broad spectrum of bacteria, such as *S. aureus*, *E. coli*, *P. aeruginosa*, *S. typhimurium*, *K. pneumoniae*, *Enterococcus faecalis*, etc. In general, it can be stated that the oxide form of the metals that possess antibacterial activity, e.g., Zn, Cu, and Zn, can exhibit similar performance.[206−208] However, a controlled dosage of CuO should be employed for biomedical applications since a higher concentration of this metal oxide can cause toxicity to mammalians and vertebrates. This is due to fabrication of ROS, which can highly damage mitochondria and deoxyribonucleic acid (DNA).[209−211] CuO-containing Nb_2O_5 films are deposited via magnetron sputtering method, where the CuO reinforcing phase can be included in the microstructure of growing Nb_2O_5 though a cosputtering route. The composite coating deposition process accomplished by sputtering Nb and Cu targets under a pure oxygen atmosphere. A smoother surface can be obtained when the CuO reinforcement is incorporated into the microstructure of pure Nb_2O_5 film. The included CuO phase can also improve the nanohardness of the pure layer from 4.78 to 7.19 GPa. Moreover, a slight increase in maximum scratch depth of coatings with CuO addition is observed. Interestingly, both J_{corr} and E_{corr} values are escalated with inclusion of CuO to a pure Nb_2O_5 layer. This means while the embedded reinforcing agent has a beneficial influence on the thermodynamic aspect of corrosion, it degrades the kinetic aspect. The mechanism(s) governing such a corrosion behavior remains to be elucidated in the published literature.[122]

Polymeric Additives. The polymeric additives, e.g., PEG and erythromycin, can be added to the pure Nb_2O_5 layers to tackle specific deficiencies or evolve new functions. The polymer-reinforced Nb_2O_5 composite layers can be deposited via magnetron sputtering and sol−gel techniques. While sputter deposition of composite coatings is carried out using composite targets,[45] to obtain sol−gel derived polymer-added Nb_2O_5 composite films it is necessary to prepare a polymer-containing sol, followed by adding the sol to the as-prepared Nb_2O_5 sol with desired ratios.[43]

PEG is a class of antifouling polymers, adopting its high antifouling performance from surface hydration and steric hindrance effects. The hydrophilic nature, low toxicity, solubility in water, and bioactivity of PEG appreciably extend its clinical applications, such as drug delivery and wound healing.[212] In drug delivery applications, PEG serves as a carrier for hydrophobic drug molecules. This can highly promote the dissolution properties and aqueous stability of the loaded drugs.[45,148] Besides, PEG can serve as a linker, which covalently binds peptides to antibacterial agents, such as gold nanoparticles.[213] While the included PEG has no noticeable effect on the phase structure of the pure Nb_2O_5 layers, an increase in surface roughness with the PEG embedment has been reported.[45] The composite coating illustrates higher bonding strength to the underlying implant than that of the pure film. It is attributed to the higher content of formed apatite throughout the coated-implant. Moreover, the composite layer that implanted *in vivo* for 2 weeks has higher adhesion strength than that of the pure layer implanted for 6 weeks, indicating the faster healing period for dental implants coated by composite film. Such an achievement brings forth promising outcomes for both patients and dentists.[148] For antibacterial applications, the Nb_2O_5-PEG composite deposit can be immersed in an antimicrobial peptide-containing medium, e.g. glycopeptide, so that the PEG acts as the linker for loading the antimicrobial peptide on the coating. The included PEG gives rise to drug delivery efficiency, thereby promoting the antibacterial activity of the coated implant against both Gram-negative and Gram-positive bacteria. However, the concentration of the incorporated antimicrobial peptide that induced acceptable antibacterial performance is different for various types of the bacteria.[45]

Erythromycin is usually employed to treat bacterial infection and can be synthesized using a strain of Streptomyces *erythreus*, which is present in soil. It shows high antibacterial efficiency against some of the Gram-positive bacteria, including listeria, streptococci, etc. Antibacterial activity of erythromycin is related to its ability to prevent protein synthesis of bacteria through binding to the 50S ribosomal element.[214−216] The antibacterial performance of sol−gel derived erythromycin-loaded Nb_2O_5 films directly depends on the dosage of the loaded antibiotic and immersion time. It may be correlated with the higher concentration of the released erythromycin at higher antibiotic dosage and/or prolonged immersion time.[43]

Summary of Properties. As it is perceived, section 4 of this review encompasses descriptions about general aspects of Nb_2O_5 coatings reinforced by various additives and attempts to provide a meaningful relationship between the processing variables, such as content of included reinforcements and parameters involved in the deposition method, and overall characteristics of the resultant composite layers. To give a better view of the influence of studied variables on the mechano-corrosion properties and wettability of the composite films, comparative tables are presented. This section not only contributes to scholars in selection of the most appropriate fabrication method, material type, and operating factors depending on necessities of the targeted application but also

Table 9. Mechanical Properties of the Particle-Strengthened Nb_2O_5 Composite Layers

type of reinforcing phase	studied variable (amount)	deposition technique	corrosive medium[a]	lowest reported j_{corr}/μA cm^{-2}	highest reported E_{corr}/mV	highest reported R_p/kΩ cm^2	refs
Cu	content of reinforcing phase; 17−25 at %	magnetron sputtering	0.5 M NaCl, 2 g/L KF; pH 2 at room temperature	0.07	9		117
Cu	composite film containing constant content of 25 at %	magnetron sputtering	0.5 M NaCl, 2 g/L KF; pH 2 at room temperature	0.07	10		140
Ce	weight percent of Ce in the prepared sols; 1−2 wt %	sol−gel	SBF	0.012	−234	297930	191
Zn	molar ratios of Nb to Zn: ranging from 0.5:0 to 0.5:0.75	sol−gel	SBF	0.07	−172	548.30	192
CuO	composite film containing constant content of CuO	magnetron sputtering	0.5 M NaCl, 2 g/L KF; pH 2 at room temperature	9.93	262		122

[a] The test temperature is a key factor affecting the results of corrosion assay. The majority of the published papers can be criticized for not reporting the accurate temperature recorded during the corrosion test since room temperature may be varied in a considerable range depending on the place and time at which the test was performed.

Table 10. Contact Angle Values of the Particle-Reinforced Nb_2O_5 Composite Coatings[a]

type of reinforcing phase	studied variable (amount)	deposition technique	used droplet type in wettability assay	the lowest reported contact angle/deg	refs
Cu	17−25 at %	magnetron sputtering	water, ethanol, ethylene glycol	7.2 ± 2.3	117
Ce	1−2 wt %	sol−gel	water	26	191
Zn	molar ratios of Nb:Zn from 0.5:0 to 0.5:0.75	sol−gel	water	26	192

[a] In accordance with reported data, the particle-reinforced Nb_2O_5 composite coatings are hydrophilic, irrespective of the fabrication method.

reveals the untreated points in this field that remain to be addressed. Table 8 and Table 9 summarize the mechanical and corrosion properties of the particle-strengthened Nb_2O_5 composite layers.

Reported results suggested that the highest value of nanohardness of the composite films is in the range of 7−8 GPa. To obtain different nanohardness and elastic modulus values, the content of included reinforcement and/or processing parameters can be changed.

The results reveal that the particle-reinforced Nb_2O_5 composite layers are generally corrosion resistant and show high corrosion performance in a variety of corrosive media. However, the importance of the test medium cannot be neglected. The contact angle values of the particle-reinforced Nb_2O_5 composite coatings are outlined in Table 10.

Nb_2O_5 as Reinforcing Phase. Nb_2O_5 carries the promise of improved morphological characteristics, hardness, corrosion resistance, bioactivity, and biocompatibility if it is added as a reinforcing phase to a matrix at the proper concentration. Usually, Nb_2O_5 is employed to strengthen the polymer layers, such as polypyrrole (PPY) and polydimethylsiloxane (PDMS).[73,110]

The surface uniformity of the electrochemically deposited PPY coatings is enhanced with the introduction of Nb_2O_5 particles. Furthermore, the size and number of present microcracks, surface roughness, and grain size decrease when Nb_2O_5 is codeposited.[110] The microstructure of sol−gel derived PDMS-Nb_2O_5 film becomes more polymorphic with an increase in the concentration of Nb_2O_5 dopant. The content of the included dopant has no positive contribution to elimination of the present microcracks.[73] The composite PPY-Nb_2O_5 layer shows higher hardness than that of pure PPY film due to the densification of the polymer matrix. Moreover, the corrosion protection efficiency of the PPY films rises with codeposition of the Nb_2O_5 phase due to increasing the localization of charge in the PPY chain and improving the surface homogeneity. The higher the included reinforcing phase, the superior the corrosion resistance. The hydrophilicity of PPY coating enhances when Nb_2O_5 is included in the deposit. This is ascribed to the hydrophilic nature of Nb_2O_5 in the polymer matrix.[110] On the other hand, there is an interesting relationship between the wettability of the PDMS-Nb_2O_5 composite layer and Nb_2O_5 concentration. The hydrophobicity of the PDMS coating is enhanced with the codeposition of Nb_2O_5 up to a certain concentration, i.e., 80%, followed by a slight decrease in contact angle value with a further rise in the concentration of Nb_2O_5 in the range of 90−100%. The enhanced hydrophobicity in the mentioned range is attributed to the formation of hybrid spheres in the structure of the deposit that enhances the surface roughness. The interesting point is that the pure Nb_2O_5 coating (100% Nb_2O_5) exhibits a hydrophilic nature. The contact angle value of pure Nb_2O_5 is less than a half and a third of pure PDMS and PDMS-80% Nb_2O_5, respectively.[73] The reported results on the effect of Nb_2O_5 concentration on the biocompatibility of polymer matrix composite deposits are different. While Kumar et al.[110] have reported a direct correlation between the amounts of loaded Nb_2O_5 and biocompatibility of the electrochemically deposited PPY-Nb_2O_5 coatings, Young et al.[73] have illustrated that the biocompatibility of PDMS-Nb_2O_5 increases with a certain amount of codeposited Nb_2O_5, i.e., 40%, followed by a decrease in the property by a further rise in Nb_2O_5 concentration up to 70%. Again, an increase in biocompatibility has been observed when Nb_2O_5 concentration is increased in the range of 70−100%. The dependence of final characteristics of a ceramic-reinforced polymer matrix composite coating to the content of the included ceramic reinforcing phase, herein Nb_2O_5, hold the promise to meet the various expectations in fabrication and applications of implants. The composite films containing low ceramic phase are suitable for soft tissue applications, while for hard tissue applications it is recommended to increase the content of Nb_2O_5 in the

Table 11. Reported Results for Contact Angle and Cell Proliferation of Nb_2O_5-Reinforced Polymer Matrix Composite Layers

coating type	deposition method	concentration of Nb_2O_5	droplet liquid used in wettability assay	lowest reported contact angle/deg	type of cultured cells	highest reported absorbance	refs
PPY-Nb_2O_5	electrochemical deposition	1−20 mg L^{-1} in the electrolyte	SBF	12.9	MG-63 osteoblast cell	≈1.1	110
PDMS-Nb_2O_5	sol−gel	20−100% in the coating	distilled water	43.4 ± 6.7	fibroblast	2.5	73

coating. Table 11 outlines the reported results for contact angle and cell proliferation of Nb_2O_5-reinforced polymer matrix composite layers.

5. CONCLUSIONS AND FUTURE HORIZONS

Surface finishing techniques and the type of materials used to modify the surface of the biomaterial have undergone unprecedented development over the past 3 decades. Niobium oxide-containing coatings are promising candidates to tackle the challenges that threaten the successful long-term use of the metallic implants. The present review paper attempts to discuss the properties, application, and market of niobium and its oxides, putting emphasis on their biomedical properties and applications. The overall characteristics of the pure Nb_xO_y and Nb_xO_y-containing coatings deposited by various surface finishing techniques will also be treated in detail, putting stress on the importance of surface finishing with pure Nb_xO_y and Nb_xO_y-containing layers along with drawing the relationship between the operating parameters and final properties of the resultant films.

In summary, pure Nb_xO_y and Nb_xO_y-containing coatings can be deposited using a variety of dry and wet techniques. The coatings greatly affect the overall characteristics of the underlying biomaterials, where the deposited layers not only address the deficiencies of the biomaterials, such as corrosion resistance but also induce some new properties, e.g., antibacterial activity. The Nb_xO_y-containing composite coatings in which the Nb_xO_y matrix is reinforced by metallic, ceramic, and polymeric additives, are developed to provide much more beneficial properties. The selection of the included reinforcing phase is highly dependent on the targeted application. However, the potential of Nb_xO_y-containing coatings is still not really being put to work for developing high-quality biomaterials used in a variety of clinical applications. Therefore, there is still much to be investigated and understood in this field. In the following text, a list of challenges and upcoming development prospects is presented in light of the status quo of Nb_xO_y-coated biomaterials and the roles that Nb_xO_y-containing coatings can play in biomedical implants.

Having reviewed the benefits and limitations of surface finishing methods, it can be readily appreciated that several approaches that can be employed to fabricate efficient Nb_xO_y-containing coatings for clinical applications. Electrodeposition, EPD, and spraying are potential techniques that may lead to uniform layers with fruitful properties. Regarding pure Nb_xO_y films, in-depth studies are needed to fully understand the effects of operating parameters for each coating technique on the final properties of the resultant layer to explicitly state how a given parameter can change the final properties. The published literature fails to address this important challenge. Moreover, studying the role of pre/post-treatments may lead to some profitable outcomes. Detailed assessments are needed to correlate the changes in mechano-corrosion and biological performance of the Nb_xO_y coated-implants with the physicochemical characteristics of the coatings caused by alteration of the reaction environment during coating deposition.

With respect to a variety of reinforcing phases, biocompatible and bioactive additives, e.g., graphene oxide, carbon nanotubes, and metal oxides, come to mind, which can potentially promote the final performance of the pure Nb_xO_y layers and/or induce new functions to them. The concept of duplex particles-reinforced Nb_xO_y coatings should attract considerable future R&D attention. Having a glance at the number of the published papers in the field of Nb_xO_y-containing composite coatings, it can be inferred that much work remains to establish reliable relationships between the type of reinforcing phases and functions of the resultant composite films. The authors believe that a more concerted focus on Nb_xO_y-containing composite coatings produced by different wet and dry techniques, in which Nb_xO_y acts as the matrix or reinforcing phase, can offer the prospect of using these coatings as the next generation of biocompatible layers in biomedical applications. The role of processing parameters in obtaining efficient Nb_xO_y-containing composite coatings should not be overlooked. The deposition of duplex particles-reinforced Nb_xO_y-containing composite coatings in which the Nb_xO_y matrix is strengthened by two reinforcing agents, and the application of interlayer(s) are two other feasible suggestions which are believed to open numerous possibilities to realize high quality Nb_xO_y-containing composite coatings.

■ AUTHOR INFORMATION

Corresponding Authors

Livia Visai − *Molecular Medicine Department (DMM), Center for Health Technologies (CHT), UdR INSTM, University of Pavia, 27100 Pavia, Italy; Medicina Clinica-Specialistica, UOR5 Laboratorio di Nanotecnologie, ICS Maugeri, IRCCS, 27100 Pavia, Italy;* orcid.org/0000-0003-1181-3632; Email: livia.visai@unipv.it

Jafar Khalil-Allafi − *Research Center for Advanced Materials, Faculty of Materials Engineering, Sahand University of Technology, 513351996 Tabriz, Iran;* orcid.org/0000-0002-3291-753X; Email: jallafi@yahoo.de

Authors

Mir Saman Safavi − *Research Center for Advanced Materials, Faculty of Materials Engineering, Sahand University of Technology, 513351996 Tabriz, Iran; Molecular Medicine Department (DMM), Center for Health Technologies (CHT), UdR INSTM, University of Pavia, 27100 Pavia, Italy*

F. C. Walsh − *Electrochemical Engineering Laboratory & National Centre for Advanced Tribology, Faculty of Engineering and the Environment, University of Southampton, Southampton SO17 1BJ, U.K.*

Complete contact information is available at:
https://pubs.acs.org/10.1021/acsomega.2c00440

Notes

The authors declare no competing financial interest.

Biographies

Mir Saman Safavi received a B.Sc. (2015) and M.Sc. (2018) from the Department of Materials Science and Engineering at University of Tabriz. During his B.Sc. and M.Sc. studies, he worked on “studying on mechanical properties of Cu-based composites” and “electrodeposition of Ni-based nanocomposite coatings”, respectively. He is a Ph.D. candidate at Sahand University of Technology, working on the surface modification of biomaterials using the electrochemical deposition technique. Mir Saman Safavi has been the author and coauthor of over 40 ISI and conference papers, which have been cited more than 440 times, giving him an H-index of 14.

F. C. Walsh is an Emeritus Professor in Electrochemical Engineering in the Department of Mechanical Engineering at the University of Southampton, U.K., where he founded the Electrochemical Engineering Laboratory He is a member of the National Centre for Advanced Tribology at Southampton and the Materials Engineering Research Group. Previous positions have included Director of the Research Institute for Industry at Southampton, Head of Chemical Engineering at the University of Bath, Head of Chemistry, Physics & Radiography then Pharmacy & Biomedical Sciences at the University of Portsmouth. He has been a Visiting Professor at the University of Wollongong and the University of Strathclyde. Frank has spent his life crossing the boundaries of chemistry, biology, materials science, and chemical engineering. He holds the qualifications of B.Sc. (Applied Chemistry), M.Sc. (Materials Protection), and Ph.D. (Electrodeposition and Electrochemical Engineering) following studies at Portsmouth, Manchester, and Loughborough Universities. He is a Chartered-Chemist, Environmentalist, Scientist, and Engineer and a Fellow of the Royal Society of Chemistry, the Institute of Mining, Materials and Metallurgy, the Institute of Materials Finishing, and the Institute of Corrosion. His R&D output, which spans the areas of energy conversion, electroactive nanomaterials, coating technology, electrochemical monitoring and sensors, corrosion, surface finishing, and electrochemical process engineering, includes 4 text books, 200 conference presentations, and over 500 research papers. Frank was awarded the Westinghouse Prize in 1999 and 2009 (best paper on metallic coatings) and the Johnson Matthey Silver Medal of the Institute of Metal Finishing in 2007 (precious metal nanoparticles inside nanotube arrays), the Breyer Medal of the Royal Australian Chemical Institute in 2000 (international contributions to electrochemical engineering and energy), the NACE Fellow honour in 2011, the Inman Medal of the UK Centre for CO_2 reduction, London (international contributions to environment and energy) in 2012, the 2017 Castner Medal of the (achievements in industrial electrochemistry), and the Gold Medal, the highest award of the Institute of Materials Finishing (lifelong contributions to electrochemical surface finishing) in 2018. In collaboration with industry, Frank has supervised over 50 Ph.D. degrees and developed/improved over 60 industrial processes.

Livia Visai is an Associate Professor in Biochemistry at the Department of Molecular Medicine (DMM), Faculty of Medicine, University of Pavia, Pavia, Italy. She is Referent of the Academic Strategic project of University of Pavia titled “Center for Health Technologies” (CHT) and Coordinator of the Nanomedicine Pillar, Pavia, Italy. She is also operating as an Associate Professor within the National Health Service of the Scientific Clinical Institutes (ICS) Maugeri, Società Benefit Spa, IRCCS, Pavia, Italy. She is coordinating a laboratory interested in studying the effect exerted by the application of nanotechnology in tissue regeneration and in bone remodeling (in particular in microgravity), in the reduction of bacterial infection, and in the diagnosis and therapy of cancer. She has more than 184 papers published in PubMed with a WoS H-index of 46.

Jafar Khalil-Allafi received a B.Sc. (1988; Isfahan University of Technology-Iran), M.Sc. (1992; Iran University of Science and Technology-Iran), and Ph.D. (2002; Ruhr University Bochum-Germany) with the highest rank. Prof. Jafar Khalil-Allafi has received international and national awards and fellowships such as the Thyssen-Krupp innovation price 2002 in Germany. He has been also the supervisor and advisor of more than 100 postgraduate theses. Prof. Jafar Khalil-Allafi has been the author and coauthor of 3 patents, 3 books, and over 100 papers which have been cited more than 3500 times, giving him an H-index of 29.

■ NOMENCLATURE

List of Symbols With Meanings and Units

E_{corr}	corrosion potential, V
j_{corr}	corrosion current density, A cm^{-2}
R_a	average surface roughness, μm
R_{ct}	charge transfer resistance, ohm
R_p	polarization resistance, ohm

Abbreviations

ALP	alkaline phosphatase activity
BCC	body cantered-cubic
CAGR	compound annual growth rate
CaP	calcium phosphate
CTE	coefficient of thermal expansion
DMEM	Dulbecco’s modified Eagle’s medium
DNA	deoxyribonucleic acid
EIS	electrochemical impedance spectroscopy
EPD	electrophoretic deposition
HAp	hydroxyapatite
HPMEC	primary human pulmonary microvascular endothelial cells
MTT	3-(4,5-dimethylthiazol-2-yl)-2,5-diphenyl-2H-tetrazolium bromide (cell viability and proliferation of cell culture assay)
PBS	phosphate buffer saline
PDMS	polydimethylsiloxane
PEG	polyethylene glycol
PEO	plasma electrolytic oxidation
PPY	polypyrrole
PU	polyurethane
RF	radio frequency
ROS	reactive oxygen species
SBF	simulated body fluid

■ REFERENCES

(1) Zimmermann, E. A.; Busse, B.; Ritchie, R. O. The fracture mechanics of human bone: influence of disease and treatment. *Bonekey Rep.* **2015**, *4*, 743.

(2) Tabatabaei, F. S.; Torres, R.; Tayebi, L. Biomedical materials in dentistry. *Applications of Biomedical Engineering in Dentistry* **2020**, 3−20.

(3) National Institutes of Health. Clinical Applications of Biomaterials. *NIH Consens. Statement* **1982**, *4*, 1−19.

(4) Hench, L. L. *An Introduction to Bioceramics*, 2nd ed.; World Scientific, 2013.

(5) Safavi, M. S.; Surmeneva, M. A.; Surmenev, R. A.; Khalil-Allafi, J. RF-magnetron sputter deposited hydroxyapatite-based composite & multilayer coatings: A systematic review from mechanical, corrosion, and biological points of view. *Ceram. Int.* **2021**, *47*, 3031−3053.

https://doi.org/10.1021/acsomega.2c00440
ACS Omega 2022, 7, 9088−9107

(6) Safavi, M. S.; Walsh, F. C.; Surmeneva, M. A.; Surmenev, R. A.; Khalil-Allafi, J. Electrodeposited Hydroxyapatite-Based Biocoatings: Recent Progress and Future Challenges. *Coatings* **2021**, *11*, 110.

(7) Shokri, N.; Safavi, M. S.; Etminanfar, M.; Walsh, F. C.; Khalil-Allafi, J. Enhanced corrosion protection of NiTi orthopedic implants by highly crystalline hydroxyapatite deposited by spin coating: The importance of pre-treatment. *Mater. Chem. Phys.* **2021**, *259*, 124041.

(8) Mohammad Salahi Tohidi, P.; Safavi, M. S.; Etminanfar, M.; Khalil-Allafi, J. Pulsed electrodeposition of compact, corrosion resistant, and bioactive HAp coatings by application of optimized magnetic field. *Mater. Chem. Phys.* **2020**, *254*, 123511.

(9) Sheykholeslami, S. O.; Fathyunes, L.; Etminanfar, M.; Khalil-Allafi, J. In-vitro biological behavior of calcium phosphate coating applied on nanostructure surface of anodized Nitinol alloy. *Mater. Res. Express.* **2019**, *6*, 095407.

(10) Fathyunes, L.; Khalil-Allafi, J.; Sheykholeslami, S. O.; Moosavifar, M. Biocompatibility assessment of graphene oxide-hydroxyapatite coating applied on TiO_2 nanotubes by ultrasound-assisted pulse electrodeposition. *Mater. Sci. Eng., C* **2018**, *87*, 10−21.

(11) Fathyunes, L.; Khalil-Allafi, J. Effect of employing ultrasonic waves during pulse electrochemical deposition on the characteristics and biocompatibility of calcium phosphate coatings. *Ultrason. Sonochem.* **2018**, *42*, 293−302.

(12) Etminanfar, M. R.; Khalil-Allafi, J.; Sheykholeslami, S. O. The effect of hydroxyapatite coatings on the passivation behavior of oxidized and unoxidized superelastic nitinol alloys. *J. Mater. Eng. Perform.* **2018**, *27*, 501−509.

(13) Mohandesnezhad, S.; Etminanfar, M.; Mahdavi, S.; Safavi, M. S. Enhanced bioactivity of 316L stainless steel with deposition of polypyrrole/hydroxyapatite layered hybrid coating: Orthopedic applications. *Surf. Interfaces* **2022**, *28*, 101604.

(14) Etminanfar, M.; Khalil-Allafi, J. On the electrodeposition of Ca-P coatings on nitinol alloy: a comparison between different surface modification methods. *J. Mater. Eng. Perform.* **2016**, *25*, 466−473.

(15) Hu, C.; Ashok, D.; Nisbet, D. R.; Gautam, V. Bioinspired surface modification of orthopedic implants for bone tissue engineering. *Biomaterials* **2019**, *219*, 119366.

(16) Holman, H.; Kavarana, M. N.; Rajab, T. K. Smart materials in cardiovascular implants: Shape memory alloys and shape memory polymers. *Artif. Organs* **2021**, *45*, 454−463.

(17) Anabtawi, M.; Thomas, M.; Lee, N. J. The use of interlocking polyetheretherketone (PEEK) patient-specific facial implants in the treatment of facial deformities. A retrospective review of ten patients. *J. Oral Maxillofac. Surg.* **2021**, *79*, 1145.e1−1145.e9.

(18) Hämmerle, C. H.; Tarnow, D. The etiology of hard-and soft-tissue deficiencies at dental implants: A narrative review. *J. Clin. Periodontol.* **2018**, *45*, S267−S277.

(19) Bundy, K. Biomaterials and the Chemical Environment of the Body. In *Joint Replacement Technology*; Woodhead Publishing Limited, 2008; pp 56−80.

(20) Pandey, A.; Awasthi, A.; Saxena, K. K. Metallic implants with properties and latest production techniques: a review. *Adv. Mater. Process. Technol.* **2020**, *6*, 405−440.

(21) Wong, K. C.; Scheinemann, P. Additive manufactured metallic implants for orthopaedic applications. *Sci. China Mater.* **2018**, *61*, 440−454.

(22) Silva-Bermudez, P.; Rodil, S. An overview of protein adsorption on metal oxide coatings for biomedical implants. *Surf. Coat. Technol.* **2013**, *233*, 147−158.

(23) Etminanfar, M. R.; Sheykholeslami, S. O.; Khalili, V.; Mahdavi, S. Biocompatibility and drug delivery efficiency of PEG-b-PCL/hydroxyapatite bilayer coatings on Nitinol superelastic alloy. *Ceram. Int.* **2020**, *46*, 12711−12717.

(24) Khalili, V.; Khalil-Allafi, J.; Xia, W.; Parsa, A. B.; Frenzel, J.; Somsen, C.; Eggeler, G. Preparing hydroxyapatite-silicon composite suspensions with homogeneous distribution of multi-walled carbon nano-tubes for electrophoretic coating of NiTi bone implant and their effect on the surface morphology. *Appl. Surf. Sci.* **2016**, *366*, 158−165.

(25) Maleki-Ghaleh, H.; Khalil-Allafi, J. Characterization, mechanical and in vitro biological behavior of hydroxyapatite-titanium-carbon nanotube composite coatings deposited on NiTi alloy by electrophoretic deposition. *Surf. Coat. Technol.* **2019**, *363*, 179−190.

(26) Bazaka, O.; Bazaka, K.; Kingshott, P.; Crawford, R. J.; Ivanova, E. P. *Metallic Implants for Biomedical Applications*. Royal Society of Chemistry, 2021; pp 1−98.

(27) Kinani, L.; Najih, R.; Chtaini, A. Corrosion inhibition of titanium in artificial saliva containing fluoride. *Leonardo J. Sci.* **2008**, *12*, 243−250.

(28) Choudhury, N.; Kannan, A.; Dutta, N. Novel Nanocomposites and Hybrids for High-Temperature Lubricating Coating Applications. In *Tribology of Polymeric Nanocomposites: Friction and Wear of Bulk Materials and Coatings*, 2nd ed.; Elsevier B.V., 2013; pp 717−778.

(29) Lison, D. Cobalt. In *Handbook on the Toxicology of Metals*; Elsevier, 2015; pp 743−763.

(30) Asghari, R.; Safavi, M. S.; Khalil-Allafi, J. A facile and cost-effective practical approach to develop clinical applications of NiTi: Fenton oxidation process. *Trans. IMF* **2020**, *98*, 250−257.

(31) Nagels, J.; Stokdijk, M.; Rozing, P. M. Stress shielding and bone resorption in shoulder arthroplasty. *J. Shoulder Elb. Surg.* **2003**, *12*, 35−39.

(32) Al-Tamimi, A. A.; Fernandes, P. R.; Peach, C.; Cooper, G.; Diver, C.; Bartolo, P. J. Metallic bone fixation implants: A novel design approach for reducing the stress shielding phenomenon. *Virtual Phys. Prototyp.* **2017**, *12*, 141−151.

(33) Zhang, E.; Xu, L.; Yu, G.; Pan, F.; Yang, K. In vivo evaluation of biodegradable magnesium alloy bone implant in the first 6 months implantation. *J. Biomed. Mater. Res.* **2009**, *90A*, 882−893.

(34) Hayashi, K.; Matsuguchi, N.; Uenoyama, K.; Sugioka, Y. Re-evaluation of the biocompatibility of bioinert ceramics in vivo. *Biomaterials* **1992**, *13*, 195−200.

(35) Kumar, S.; Simpson, D.; Smart, R. S. C. Plasma processing for inducing bioactivity in stainless steel orthopaedic screws. *Surf. Coat. Technol.* **2007**, *202*, 1242−1246.

(36) MacDonald, D. E.; Deo, N.; Markovic, B.; Stranick, M.; Somasundaran, P. Adsorption and dissolution behavior of human plasma fibronectin on thermally and chemically modified titanium dioxide particles. *Biomaterials* **2002**, *23*, 1269−1279.

(37) Tambasco de Oliveira, P.; Nanci, A. Nanotexturing of titanium-based surfaces upregulates expression of bone sialoprotein and osteopontin by cultured osteogenic cells. *Biomaterials* **2004**, *25*, 403−413.

(38) Lossdörfer, S.; Schwartz, Z.; Wang, L.; Lohmann, C. H.; Turner, J. D.; Wieland, M.; Cochran, D. L.; Boyan, B. D. Microrough implant surface topographies increase osteogenesis by reducing osteoclast formation and activity. *J. Biomed. Mater. Res.* **2004**, *70A*, 361−369.

(39) Shahryari, A.; Azari, F.; Vali, H.; Omanovic, S. The response of fibrinogen, platelets, endothelial and smooth muscle cells to an electrochemically modified SS316LS surface: Towards the enhanced biocompatibility of coronary stents. *Acta Biomater.* **2010**, *6*, 695−701.

(40) Horandghadim, N.; Khalil-Allafi, J.; Urgen, M. Effect of Ta_2O_5 content on the osseointegration and cytotoxicity behaviors in hydroxyapatite-Ta_2O_5 coatings applied by EPD on superelastic NiTi alloys. *Mater. Sci. Eng., C* **2019**, *102*, 683−695.

(41) Pham, V. T. H.; Truong, V. K.; Orlowska, A.; Ghanaati, S.; Barbeck, M.; Booms, P.; Fulcher, A. J.; Bhadra, C. M.; Buividas, R.; Baulin, V.; Kirkpatrick, C. J.; Doran, P.; Mainwaring, D. E.; Juodkazis, S.; Crawford, R. J.; Ivanova, E. P. Race for the surface": eukaryotic cells can win. *ACS Appl. Mater. Interfaces* **2016**, *8*, 22025−22031.

(42) Subbiahdoss, G.; Kuijer, R.; Grijpma, D. W.; van der Mei, H. C.; Busscher, H. J. Microbial biofilm growth vs. tissue integration:"the race for the surface" experimentally studied. *Acta Biomater.* **2009**, *5*, 1399−1404.

(43) Pradhan, D.; Wren, A.; Mellott, N. A preliminary study into the efficacy of antibiotic doped niobium oxide coatings on 316L prepared by incipient wetness impregnation and sol-gel synthesis. *Mater. Lett.* **2017**, *190*, 150−153.

(44) Antoci, V., Jr; Adams, C. S.; Parvizi, J.; Davidson, H. M.; Composto, R. J.; Freeman, T. A.; Wickstrom, E.; Ducheyne, P.; Jungkind, D.; Shapiro, I. M.; Hickok, N. J. The inhibition of Staphylococcus epidermidis biofilm formation by vancomycin-modified titanium alloy and implications for the treatment of periprosthetic infection. *Biomaterials* **2008**, *29*, 4684−4690.

(45) Khalaf, H.; Hussien, B.; Alzubaidi, T. Anti-bacterial evaluation of biocomposite coated dental implant after immersion in glycopeptide. *Indian J. Nat. Sci.* **2018**, *8*, 49.

(46) Ahmadiyan, S.; Khalil-Allafi, J.; Etminanfar, M. R.; Safavi, M. S.; Hosseini, M. Antibacterial activity and biocompatibility of Ag-coated Ti implants: importance of surface modification parameters. *Trans. IMF* **2022**, 1−10.

(47) Safavi, M. S.; Etminanfar, M. A review on the prevalent fabrication methods, microstructural, mechanical properties, and corrosion resistance of nanostructured hydroxyapatite containing bilayer and multilayer coatings used in biomedical applications. *J. Ultrafine Grained Nanostruct. Mater.* **2019**, *52*, 1−17.

(48) Abdal-hay, A.; Barakat, N. A.; Lim, J. K. Hydroxyapatite-doped poly (lactic acid) porous film coating for enhanced bioactivity and corrosion behavior of AZ31 Mg alloy for orthopedic applications. *Ceram. Int.* **2013**, *39*, 183−195.

(49) Moskalewicz, T.; Seuss, S.; Boccaccini, A. R. Microstructure and properties of composite polyetheretherketone/Bioglass coatings deposited on Ti-6Al-7Nb alloy for medical applications. *Appl. Surf. Sci.* **2013**, *273*, 62−67.

(50) Surmenev, R. A.; Surmeneva, M. A. A critical review of decades of research on calcium phosphate-based coatings: How far are we from their widespread clinical application? *Curr. Opin. Biomed. Eng.* **2019**, *10*, 35−44.

(51) Surmenev, R. A.; Surmeneva, M. A.; Ivanova, A. A. Significance of calcium phosphate coatings for the enhancement of new bone osteogenesis-a review. *Acta Biomater.* **2014**, *10*, 557−579.

(52) Surmenev, R. A.; Ivanova, A. A.; Epple, M.; Pichugin, V. F.; Surmeneva, M. A. Physical principles of radio-frequency magnetron sputter deposition of calcium-phosphate-based coating with tailored properties. *Surf. Coat. Technol.* **2021**, *413*, 127098.

(53) Surmenev, R. A.; Grubova, I. Y.; Neyts, E.; Teresov, A. D.; Koval, N. N.; Epple, M.; Tyurin, A. I.; Pichugin, V. F.; Chaikina, M. V.; Surmeneva, M. A. Ab initio calculations and a scratch test study of RF-magnetron sputter deposited hydroxyapatite and silicon-containing hydroxyapatite coatings. *Surf. Interfaces* **2020**, *21*, 100727.

(54) Hu, R.; Lin, C.; Shi, H.; Wang, H. Electrochemical deposition mechanism of calcium phosphate coating in dilute Ca-P electrolyte system. *Mater. Chem. Phys.* **2009**, *115*, 718−723.

(55) Robertson, S. F.; Bandyopadhyay, A.; Bose, S. Titania nanotube interface to increase adhesion strength of hydroxyapatite sol-gel coatings on Ti-6Al-4V for orthopedic applications. *Surf. Coat. Technol.* **2019**, *372*, 140−147.

(56) Qi, J.; Yang, Y.; Zhou, M.; Chen, Z.; Chen, K. Effect of transition layer on the performance of hydroxyapatite/titanium nitride coating developed on Ti-6Al-4V alloy by magnetron sputtering. *Ceram. Int.* **2019**, *45*, 4863−4869.

(57) Ke, D.; Vu, A. A.; Bandyopadhyay, A.; Bose, S. Compositionally graded doped hydroxyapatite coating on titanium using laser and plasma spray deposition for bone implants. *Acta Biomater.* **2019**, *84*, 414−423.

(58) Zhang, Q.; Leng, Y.; Xin, R. A comparative study of electrochemical deposition and biomimetic deposition of calcium phosphate on porous titanium. *Biomaterials* **2005**, *26*, 2857−2865.

(59) Drevet, R.; Velard, F.; Potiron, S.; Laurent-Maquin, D.; Benhayoune, H. In vitro dissolution and corrosion study of calcium phosphate coatings elaborated by pulsed electrodeposition current on Ti6Al4V substrate. *J. Mater. Sci.: Mater. Med.* **2011**, *22*, 753−761.

(60) Jiang, J. Y.; Xu, J. L.; Liu, Z. H.; Deng, L.; Sun, B.; Liu, S. D.; Wang, L.; Liu, H. Y. Preparation, corrosion resistance and hemocompatibility of the superhydrophobic TiO$_2$ coatings on biomedical Ti-6Al-4V alloys. *Appl. Surf. Sci.* **2015**, *347*, 591−595.

(61) Kaliaraj, G. S.; Vishwakarma, V.; Alagarsamy, K.; Kamalan Kirubaharan, A.M. Biological and corrosion behavior of m-ZrO$_2$ and t-ZrO$_2$ coated 316L SS for potential biomedical applications. *Ceram. Int.* **2018**, *44*, 14940−14946.

(62) Singh, A.; Singh, S. ZnO nanowire-coated hydrophobic surfaces for various biomedical applications. *Bull. Mater. Sci.* **2018**, *41*, 94.

(63) Dinu, M.; Braic, L.; Padmanabhan, S. C.; Morris, M. A.; Titorencu, I.; Pruna, V.; Parau, A.; Romanchikova, N.; Petrik, L. F.; Vladescu, A. Characterization of electron beam deposited Nb$_2$O$_5$ coatings for biomedical applications. *J. Mech. Behav. Biomed. Mater.* **2020**, *103*, 103582.

(64) Milošev, I.; Levašič, V.; Kovač, S.; Sillat, T.; Virtanen, S.; Tiainen, V. M.; Trebše, R. Metals for Joint Replacement. In *Joint Replacement Technology*; Elsevier, 2021; pp 65−122.

(65) Catledge, S. A.; Vohra, Y. K.; Bellis, S. L.; Sawyer, A. A. Mesenchymal stem cell adhesion and spreading on nanostructured biomaterials. *J. Nanosci. Nanotechnol.* **2004**, *4*, 986−989.

(66) Ratner, B. D.; Zhang, G. A History of Biomaterials. In *Biomaterials Science*; Elsevier, 2020; pp 21−34.

(67) Allo, B. A.; Costa, D. O.; Dixon, S. J.; Mequanint, K.; Rizkalla, A. S. Bioactive and biodegradable nanocomposites and hybrid biomaterials for bone regeneration. *J. Funct. Biomater.* **2012**, *3*, 432−463.

(68) Tennese, W.; Cahoon, J. Sensitization" still a problem in the intergranular corrosion of stainless steel surgical implants. *Trends Biomater. Artif. Organs* **1973**, *1*, 635−645.

(69) Sittig, C.; Hahner, G.; Marti, A.; Textor, M.; Spencer, N. D.; Hauert, R. The implant material, Ti6Al7Nb: surface microstructure, composition and properties. *J. Mater. Sci. Mater. Med.* **1999**, *10*, 191−198.

(70) Shilder, S. Tantalum and niobium as potential prosthetic materials. *Biomaterials* **1982**, *13-10*, 1982.

(71) Ward, L.; Datta, P. K. Physical Properties of Nb Coatings for Biomedical Applications. *Key Eng. Mater.* **1992**, *72*, 505−522.

(72) Leitune, V. C.; Collares, F. M.; Takimi, A.; de Lima, G. B.; Petzhold, C. L.; Bergmann, C. P.; Samuel, S. M. Niobium pentoxide as a novel filler for dental adhesive resin. *J. Dent.* **2013**, *41*, 106−113.

(73) Young, M. D.; Tran, N.; Tran, P. A.; Jarrell, J. D.; Hayda, R. A.; Born, C. T. Niobium oxide-polydimethylsiloxane hybrid composite coatings for tuning primary fibroblast functions. *J. Biomed. Mater. Res.* **2014**, *102*, 1478−1485.

(74) Velten, D.; Eisenbarth, E.; Schanne, N.; Breme, J. Biocompatible Nb$_2$O$_5$ thin films prepared by means of the sol-gel process. *J. Mater. Sci. Mater. Med.* **2004**, *15*, 457−461.

(75) Wirth, J.; Tayebi, L. Engineering of Dental Titanium Implants and Their Coating Techniques. In *Applications of Biomedical Engineering in Dentistry*; Springer, 2020; pp 149−160.

(76) Pauline, S. A.; Rajendran, N. Corrosion behaviour and biocompatibility of nanoporous niobium incorporated titanium oxide coating for orthopaedic applications. *Ceram. Int.* **2017**, *43*, 1731−1739.

(77) Zhang, S.; Cheng, X.; Yao, Y.; Wei, Y.; Han, C.; Shi, Y.; Wei, Q.; Zhang, Z. Porous niobium coatings fabricated with selective laser melting on titanium substrates: preparation, characterization, and cell behavior. *Mater. Sci. Eng., C* **2015**, *53*, 50−59.

(78) Saranya, K.; Thirupathi Kumara Raja, S.; Subhasree, R.S.; Gnanamani, A.; Das, S. K.; Rajendran, N. Fabrication of nanoporous sodium niobate coating on 316L SS for orthopaedics. *Ceram. Int.* **2017**, *43*, 11569−11579.

(79) Shi, K.; Zhang, Y.; Zhang, J.; Xie, Z. Electrochemical properties of niobium coating for biomedical application. *Coatings* **2019**, *9*, 546.

(80) Babaei, K.; Fattah-alhosseini, A.; Chaharmahali, R. A review on plasma electrolytic oxidation (PEO) of niobium: Mechanism, properties and applications. *Surf. Interfaces* **2020**, *21*, 100719.

(81) Stojadinović, S.; Tadić, N.; Radić, N.; Stefanov, P.; Grbić, B.; Vasilić, R. Anodic luminescence, structural, photoluminescent, and photocatalytic properties of anodic oxide films grown on niobium in phosphoric acid. *Appl. Surf. Sci.* **2015**, *355*, 912−920.

(82) Chi-Hsiun Kuo, P.; Chou, H.-H.; Lin, Y.-H.; Peng, P.-W.; Ou, K.-L.; Lee, W.-R. Effects of surface functionalization on the nanostructure and biomechanical properties of binary titanium-niobium alloys. *J. Electrochem. Soc.* **2012**, *159*, No. E103.

(83) Matsuno, H.; Yokoyama, A.; Watari, F.; Uo, M.; Kawasaki, T. Biocompatibility and osteogenesis of refractory metal implants, titanium, hafnium, niobium, tantalum and rhenium. *Biomaterials* **2001**, *22*, 1253−1262.

(84) Hryniewicz, T.; Rokosz, K.; Sandim, H. Z. SEM/EDX and XPS studies of niobium after electropolishing. *Appl. Surf. Sci.* **2012**, *263*, 357−361.

(85) Niinomi, M. Recent metallic materials for biomedical applications. *Metall. Mater. Trans. A* **2002**, *33*, 477.

(86) Ge, J.; Wang, F.; Xu, Z.; Shen, X.; Gao, C.; Wang, D.; Hu, G.; Gu, J.; Tang, T.; Wei, J. Influences of niobium pentoxide on roughness, hydrophilicity, surface energy and protein absorption, and cellular responses to PEEK based composites for orthopedic applications. *J. Mater. Chem. B* **2020**, *8*, 2618−2626.

(87) Samudrala, R.; Abdul Azeem, P.; Penugurti, V.; Manavathi, B. In vitro evaluation of niobia added soda lime borosilicate bioactive glasses. *J. Alloys Compd.* **2018**, *764*, 1072−1078.

(88) Canepa, P.; Ghiara, G.; Spotorno, R.; Canepa, M.; Cavalleri, O. Structural vs. electrochemical investigation of niobium oxide layers anodically grown in a Ca and P containing electrolyte. *J. Alloys Compd.* **2021**, *851*, 156937.

(89) Johansson, C.; Albrektsson, T. A removal torque and histomorphometric study of commercially pure niobium and titanium implants in rabbit bone. *Clin. Oral Implants Res.* **1991**, *2*, 24−29.

(90) Nascimento, W. J.; Bonadio, T. G.; Freitas, V. F.; Weinand, W. R.; Baesso, M. L.; Lima, W. M. Nanostructured Nb_2O_5-natural hydroxyapatite formed by the mechanical alloying method: A bulk composite. *Mater. Chem. Phys.* **2011**, *130* (1−2), 84−89.

(91) de Almeida Bino, M. C.; Eurídice, W. A.; Gelamo, R. V.; Leite, N. B.; da Silva, M. V.; de Siervo, A.; Pinto, M. R.; de Almeida Buranello, P. A.; Moreto, J. A. Structural and morphological characterization of Ti6Al4V alloy surface functionalization based on Nb_2O_5 thin film for biomedical applications. *Appl. Surf. Sci.* **2021**, *557*, 149739.

(92) Alves, A. R.; Coutinho, A.d.R. The evolution of the niobium production in Brazil. *Mater. Res.* **2015**, *18*, 106−112.

(93) Schulz, K. J., DeYoung, J. H., Seal, R. R.; Bradley, D. C., Eds. *Critical Mineral Resources of the United States: Economic and Environmental Geology and Prospects for Future Supply*, Geological Survey, 2018.

(94) Nikishina, E.; Drobot, D.; Lebedeva, E. Niobium and tantalum: State of the world market, fields of application, and raw sources. Part I. *Russ. J. Non-Ferr. Met.* **2013**, *54*, 446−452.

(95) Vandrovcova, M.; Jirka, I.; Novotna, K.; Lisa, V.; Frank, O.; Kolska, Z.; Stary, V.; Bacakova, L. Interaction of human osteoblast-like Saos-2 and MG-63 cells with thermally oxidized surfaces of a titanium-niobium alloy. *PloS one* **2014**, *9*, No. e100475.

(96) Jirka, I.; Vandrovcová, M.; Frank, O.; Tolde, Z.; Plšek, J.; Luxbacher, T.; Bačáková, L.; Starý, V. On the role of Nb-related sites of an oxidized β-TiNb alloy surface in its interaction with osteoblast-like MG-63 cells. *Mater. Sci. Eng., C* **2013**, *33*, 1636−1645.

(97) Robin, A.; Rosa, J. L. Corrosion behavior of niobium, tantalum and their alloys in hot hydrochloric and phosphoric acid solutions. *Int. J. Refract. Hard Met.* **2000**, *18*, 13−21.

(98) Covino, B. S., Jr.; Carter, J. P.; Cramer, S. D. The corrosion behavior of niobium in hydrochloric acid solutions. *Corrosion* **1980**, *36*, 554−558.

(99) Manam, N. S.; Harun, W. S.; Shri, D. N.; Ghani, S. A.; Kurniawan, T.; Ismail, M. H.; Ibrahim, M. H. Study of corrosion in biocompatible metals for implants: A review. *J. Alloys Compd.* **2017**, *701*, 698−715.

(100) Masse, J. P.; Szymanowski, H.; Zabeida, O.; Amassian, A.; Klemberg-Sapieha, J. E.; Martinu, L. Stability and effect of annealing on the optical properties of plasma-deposited Ta_2O_5 and Nb_2O_5 films. *Thin Solid Films* **2006**, *515*, 1674−1682.

(101) Ramírez, G.; Rodil, S. E.; Muhl, S.; Turcio-Ortega, D.; Olaya, J. J.; Rivera, M.; Camps, E.; Escobar-Alarcón, L. Amorphous niobium oxide thin films. *J. Non Cryst. Solids* **2010**, *356*, 2714−2721.

(102) Usha, N.; Sivakumar, R.; Sanjeeviraja, C.; Arivanandhan, M. Niobium pentoxide (Nb_2O_5) thin films: rf Power and substrate temperature induced changes in physical properties. *Optik (Stuttg.)* **2015**, *126*, 1945−1950.

(103) Lee, S. H.; Kwon, J. D.; Ahn, J. H.; Park, J. S. Compositional and electrical modulation of niobium oxide thin films deposited by plasma-enhanced atomic layer deposition. *Ceram. Int.* **2017**, *43*, 6580−6584.

(104) Marques, C.; Louro, L. H. L.; Prado da Silva, M. H. Bioactive ceramics based on Nb_2O_5 and Ta_2O_5. *Key Eng. Mater.* **2008**, *396-398*, 641−644.

(105) Amaravathy, P.; Sowndarya, S.; Sathyanarayanan, S.; Rajendran, N. Novel sol gel coating of Nb_2O_5 on magnesium alloy for biomedical applications. *Surf. Coat. Technol.* **2014**, *244*, 131−141.

(106) Marins, N. H.; Lee, B. EJ.; e Silva, R. M.; Raghavan, A.; Villarreal Carreno, N. L.; Grandfield, K. Niobium pentoxide and hydroxyapatite particle loaded electrospun polycaprolactone/gelatin membranes for bone tissue engineering. *Colloids Surf., B* **2019**, *182*, 110386.

(107) Demirkol, N.; Oktar, F. N.; Kayali, E. S. Influence of niobium oxide on the mechanical properties of hydroxyapatite. *Key Eng. Mater.* **2012**, *529-530*, 29−33.

(108) Turan, M.; Demirkol, N. Comparison of mechanical and bioactivity properties of nano hydroxyapatite-magnesium oxide and nano hydroxyapatite-niobium (V) oxide biocomposites. *Adv. Nano-Bio. Mater. Dev.* **2013**, *3*, 521−527.

(109) Li, Y.; Munir, K. S.; Lin, J.; Wen, C. Titanium-niobium pentoxide composites for biomedical applications. *Bioact. Mater.* **2016**, *1*, 127−131.

(110) Madhan Kumar, A.; Nagarajan, S.; Ramakrishna, S.; Sudhagar, P.; Kang, Y. S.; Kim, H.; Gasem, Z. M.; Rajendran, N. Electrochemical and in vitro bioactivity of polypyrrole/ceramic nanocomposite coatings on 316L SS bio-implants. *Mater. Sci. Eng., C* **2014**, *43*, 76−85.

(111) Rani, R. A.; Zoolfakar, A. S.; O'Mullane, A. P.; Austin, M. W.; Kalantar-Zadeh, K. Thin films and nanostructures of niobium pentoxide: fundamental properties, synthesis methods and applications. *J. Mater. Chem. A* **2014**, *2*, 15683−15703.

(112) Singh, C.; Pandey, M. K.; Biradar, A. M.; Srivastava, A. K.; Sumana, G. A bienzyme-immobilized highly efficient niobium oxide nanorod platform for biomedical application. *RSC Adv.* **2014**, *4*, 15458−15465.

(113) Holtzberg, F.; Reisman, A.; Berry, M.; Berkenblit, M. Chemistry of the group VB pentoxides. VI. The polymorphism of Nb_2O_5. *J. Am. Chem. Soc.* **1957**, *79*, 2039−2043.

(114) Schäfer, H.; Gruehn, R.; Schulte, F. The modifications of niobium pentoxide. *Angew. Chem., Int. Ed.* **1966**, *5*, 40−52.

(115) Guerreiro Tanomaru, J. M.; Storto, I.; Da Silva, G. F.; Bosso, R.; Costa, B. C.; Bernardi, M. I.; Tanomaru-Filho, M. Radiopacity, pH and antimicrobial activity of Portland cement associated with micro- and nanoparticles of zirconium oxide and niobium oxide. *Dent. Mater. J.* **2014**, *33*, 466−470.

(116) Viapiana, R.; Flumignan, D. L.; Guerreiro-Tanomaru, J. M.; Camilleri, J.; Tanomaru-Filho, M. Physicochemical and mechanical properties of zirconium oxide and niobium oxide modified P ortland cement-based experimental endodontic sealers. *Int. Endod. J.* **2014**, *47*, 437−448.

(117) Mazur, M.; Kalisz, M.; Wojcieszak, D.; Grobelny, M.; Mazur, P.; Kaczmarek, D.; Domaradzki, J. Determination of structural, mechanical and corrosion properties of Nb_2O_5 and (NbyCu1- y) Ox thin films deposited on Ti6Al4V alloy substrates for dental implant applications. *Mater. Sci. Eng., C* **2015**, *47*, 211−221.

(118) Karlinsey, R. L.; Hara, A. T.; Yi, K.; Duhn, C. W. Bioactivity of novel self-assembled crystalline Nb2O5 microstructures in simulated and human salivas. *Biomed. Mater.* **2006**, *1*, 16.

(119) Pradhan, D.; Wren, A. W.; Misture, S. T.; Mellott, N. P. Investigating the structure and biocompatibility of niobium and titanium oxides as coatings for orthopedic metallic implants. *Mater. Sci. Eng., C* **2016**, *58*, 918−926.

(120) Pereira, B. L.; Lepienski, C. M.; Mazzaro, I.; Kuromoto, N. K. Apatite grown in niobium by two-step plasma electrolytic oxidation. *Mater. Sci. Eng., C* **2017**, *77*, 1235−1241.

(121) Eisenbarth, E.; Velten, D.; Müller, M.; Thull, R.; Breme, J. Nanostructured niobium oxide coatings influence osteoblast adhesion. *J. Biomed. Mater. Res.* **2006**, *79A*, 166−175.

(122) Grobelny, M.; Kalisz, M.; Mazur, M.; Wojcieszak, D.; Kaczmarek, D. A.; Domaradzki, J. A.; Świniarski, M.; Mazur, P. Functional Nb_2O_5 film and Nb_2O_5+ CuO, Nb_2O_5+ Graphene, Nb_2O_5+ CuO+ Graphene composite films to modify the properties of Ti6Al4V titanium alloy. *Thin Solid Films* **2016**, *616*, 64−72.

(123) Moreto, J. A.; Gelamo, R. V.; da Silva, M. V.; Steffen, T. T.; de Oliveira, C. J.; de Almeida Buranello, P. A.; Pinto, M. R. New insights of Nb_2O_5-based coatings on the 316L SS surfaces: enhanced biological responses. *J. Mater. Sci.: Mater. Med.* **2021**, *32*, 25.

(124) Orozco-Hernández, G.; Durán, P. G.; Aperador, W. Tribocorrosion Evaluation of Nb_2O_5, TiO_2, and Nb_2O_5+ TiO_2 Coatings for Medical Applications. *Lubricants* **2021**, *9*, 49.

(125) Velten, D.; Eisenbarth, E.; Winter, S.; Schanne, N.; Breme, J. Biomedical Oxide Coatings on Ti-alloys prepared by means of the Sol-Gel Process. *BioNanoMaterials* **2005**, *6* (1), 22−28.

(126) Pauline, S. A.; Rajendran, N. Biomimetic novel nanoporous niobium oxide coating for orthopaedic applications. *Appl. Surf. Sci.* **2014**, *290*, 448−457.

(127) Nagarajan, S.; Raman, V.; Rajendran, N. Synthesis and electrochemical characterization of porous niobium oxide coated 316L SS for orthopedic applications. *Mater. Chem. Phys.* **2010**, *119*, 363−366.

(128) Rafieerad, A. R.; Bushroa, A. R.; Nasiri-Tabrizi, B.; Vadivelu, J.; Yusof, F.; Baradaran, S. Graphene oxide modified anodic ternary nanobioceramics on Ti6Al7Nb alloy for orthopedic and dental applications. *Procedia Eng.* **2017**, *184*, 409−417.

(129) Mohseni, E.; Zalnezhad, E.; Bushroa, A. R. Comparative investigation on the adhesion of hydroxyapatite coating on Ti-6Al-4V implant: A review paper. *Int. J. Adhes. Adhes.* **2014**, *48*, 238−257.

(130) Priyadarshini, B.; Rama, M.; Chetan, S.; Vijayalakshmi, U. Bioactive coating as a surface modification technique for biocompatible metallic implants: a review. *J. Asian Ceram. Soc.* **2019**, *7*, 397−406.

(131) Aliofkhazraei, M.; Macdonald, D.D.; Matykina, E.; Parfenov, E.V.; Egorkin, V.S.; Curran, J.A.; Troughton, S.C.; Sinebryukhov, S.L.; Gnedenkov, S.V.; Lampke, T.; Simchen, F.; Nabavi, H.F. Review of plasma electrolytic oxidation of titanium substrates: Mechanism, properties, applications and limitations. *Appl. Surf. Sci. Adv.* **2021**, *5*, 100121.

(132) Raj, V.; Rajaram, M. P.; Balasubramanian, G.; Vincent, S.; Kanagaraj, D. Pulse anodizing—an overview. *Trans. IMF* **2003**, *81*, 114−121.

(133) Safavi, M. S.; Fathi, M.; Charkhesht, V.; Jafarpour, M.; Ahadzadeh, I. Electrodeposition of Co-P coatings reinforced by MoS_2+Y_2O_3 hybrid ceramic nanoparticles for corrosion-resistant applications: influences of operational parameters. *Metall. Mater. Trans. A* **2020**, *51*, 6740−6758.

(134) Fathi, M.; Safavi, M. S.; Mahdavi, S.; Mirzazadeh, S.; Charkhesht, V.; Mardanifar, A.; Mehdipour, M. Co-P alloy matrix composite deposits reinforced by nano-MoS_2 solid lubricant: An alternative tribological coating to hard chromium coatings. *Tribol. Int.* **2021**, *159*, 106956.

(135) Khalil-Allafi, J.; Daneshvar, H.; Safavi, M. S.; Khalili, V. A survey on crystallization kinetic behavior of direct current magnetron sputter deposited NiTi thin films. *Phys. B: Condens. Matter.* **2021**, *615*, 413086.

(136) Safavi, M. S.; Walsh, F. C. Electrodeposited Co-P alloy and composite coatings: A review of progress towards replacement of conventional hard chromium deposits. *Surf. Coat. Technol.* **2021**, *422*, 127564.

(137) Safavi, M. S.; Fathi, M.; Ahadzadeh, I. Feasible strategies for promoting the mechano-corrosion performance of Ni-Co based coatings: Which one is better? *Surf. Coat. Technol.* **2021**, *420*, 127337.

(138) Senocak, T. C.; Ezirmik, K. V.; Aysin, F.; Simsek Ozek, N.; Cengiz, S. Niobium-oxynitride coatings for biomedical applications: Its antibacterial effects and in-vitro cytotoxicity. *Mater. Sci. Eng., C* **2021**, *120*, 111662.

(139) Kalisz, M.; Grobelny, M.; Mazur, M.; Zdrojek, M.; Wojcieszak, D.; Świniarski, M.; Judek, J.; Kaczmarek, D. Comparison of mechanical and corrosion properties of graphene monolayer on Ti-Al-V and nanometric Nb_2O_5 layer on Ti-Al-V alloy for dental implants applications. *Thin Solid Films* **2015**, *589*, 356−363.

(140) Kalisz, M.; Grobelny, M.; Mazur, M.; Wojcieszak, D.; Świniarski, M.; Zdrojek, M.; Domaradzki, J.; Kaczmarek, D. Mechanical and electrochemical properties of Nb_2O_5, Nb_2O_5: Cu and graphene layers deposited on titanium alloy (Ti6Al4V). *Surf. Coat. Technol.* **2015**, *271*, 92−99.

(141) Brinker, C. J.; Lu, Y.; Sellinger, A.; Fan, H. Evaporation-induced self-assembly: nanostructures made easy. *Adv. Mater.* **1999**, *11*, 579−585.

(142) Torre, G. C.-d. l.; Espinosa-Medina, M. A.; Martinez-Villafane, A.; Gonzalez-Rodriguez, J. G.; Castano, V. M. Study of ceramic and hybrid coatings produced by the sol-gel method for corrosion protection. *Open Corros. J.* **2009**, *2*, 197−203.

(143) Nijhawan, S.; Bali, P.; Gupta, V. The international J. of oral implantology and clinical research. *Int. J. Oral Implant. Clin. Res.* **2010**, *1*, 77−82.

(144) Karlinsey, R. L. Preparation of self-organized niobium oxide microstructures via potentiostatic anodization. *Electrochem. Commun.* **2005**, *7*, 1190−1194.

(145) Karlinsey, R. L. Self-assembled Nb_2O_5 microcones with tailored crystallinity. *J. Mater. Sci.* **2006**, *41*, 5017−5020.

(146) Mackey, A. C.; Karlinsey, R. L.; Chu, T. M.; MacPherson, M.; Alge, D. L. Development of niobium oxide coatings on sand-blasted titanium alloy dental implants. *Mater. Sci. Appl.* **2012**, *3* (5), 301−305.

(147) Lokeshkumar, E.; Manojkumar, P.; Saikiran, A.; Premchand, C.; Hariprasad, S.; Rameshbabu, N. Fabrication of Ca and P containing niobium oxide ceramic coatings on niobium by PEO coupled EPD process. *Surf. Coat. Technol.* **2021**, *416*, 127161.

(148) Khalaf, H. A.; Hussien, B. M.; Al Zubaidi, T. L. Influence of Antimicrobial Bio-Composite Coating on Osseointegration of Dental Implant. *Health Sci.* **2018**, *7* (7), 110−118.

(149) Ramírez, G.; Rodil, S. E.; Arzate, H.; Muhl, S.; Olaya, J. J. Niobium based coatings for dental implants. *Appl. Surf. Sci.* **2011**, *257*, 2555−2559.

(150) Ye, Y.; Lim, R.; White, J. M. High mobility amorphous zinc oxynitride semiconductor material for thin film transistors. *J. Appl. Phys.* **2009**, *106*, 074512.

(151) Safavi, M. S.; Rasooli, A.; Sorkhabi, F. Electrodeposition of Ni-P/Ni-Co-Al_2O_3 duplex nanocomposite coatings: towards improved mechanical and corrosion properties. *Trans. IMF* **2020**, *98*, 320−327.

(152) Fathi, M.; Safavi, M. S.; Mirzazadeh, S.; Ansariyan, A.; Ahadzadeh, I. A promising horizon in mechanical and corrosion properties improvement of Ni-Mo coatings through incorporation of Y_2O_3 nanoparticles. *Metall. Mater. Trans. A* **2020**, *51*, 897−908.

(153) Rasooli, A.; Safavi, M. S.; Ahmadiyeh, S.; Jalali, A. Evaluation of TiO_2 Nanoparticles Concentration and Applied Current Density Role in Determination of Microstructural, Mechanical, and Corrosion Properties of Ni-Co Alloy Coatings. *Prot. Met. Phys. Chem. Surf.* **2020**, *56*, 320−327.

(154) Ross, J. R. *Contemporary Catalysis: Fundamentals and Current Applications*; Elsevier, 2018.

(155) Eisenbarth, E.; Velten, D.; Breme, J. Biomimetic implant coatings. *Biomol. Eng.* **2007**, *24*, 27−32.

(156) Li, J.; Jansen, J. A.; Walboomers, X. F.; van den Beucken, J. J. Mechanical aspects of dental implants and osseointegration: A narrative review. *J. Mech. Behav. Biomed. Mater.* **2020**, *103*, 103574.

(157) Prakasam, M.; Locs, J.; Salma-Ancane, K.; Loca, D.; Largeteau, A.; Berzina-Cimdina, L. Biodegradable materials and metallic implants—a review. *J. Funct. Biomater.* **2017**, *8*, 44.

(158) Cosson, M.; Debodinance, P.; Boukerrou, M.; Chauvet, M. P.; Lobry, P.; Crépin, G.; Ego, A. Mechanical properties of synthetic implants used in the repair of prolapse and urinary incontinence in women: which is the ideal material? *Int. Urogynecol. J.* **2003**, *14*, 169−178.

(159) Sumner, D. Long-term implant fixation and stress-shielding in total hip replacement. *J. Biomech.* **2015**, *48*, 797−800.

(160) Lai, Y. S.; Chen, W. C.; Huang, C. H.; Cheng, C. K.; Chan, K. K.; Chang, T. K. The effect of graft strength on knee laxity and graft in-situ forces after posterior cruciate ligament reconstruction. *PLoS One* **2015**, *10*, No. e0127293.

(161) Swain, S.; Misra, R. D.; You, C. K.; Rautray, T. R. TiO_2 nanotubes synthesised on Ti-6Al-4V ELI exhibits enhanced osteogenic activity: A potential next-generation material to be used as medical implants. *Mater. Technol.* **2021**, *36*, 393−399.

(162) Karacan, I.; Ben-Nissan, B.; Wang, H. A.; Juritza, A.; Swain, M. V.; Müller, W. H.; Chou, J.; Stamboulis, A.; Macha, I. J.; Taraschi, V. Mechanical testing of antimicrobial biocomposite coating on metallic medical implants as drug delivery system. *Mater. Sci. Eng., C* **2019**, *104*, 109757.

(163) Ibrahim, M. Z.; Sarhan, A. A.; Kuo, T. Y.; Yusof, F.; Hamdi, M.; Lee, T. M. Developing a new laser cladded FeCrMoCB metallic glass layer on nickel-free stainless-steel as a potential superior wear-resistant coating for joint replacement implants. *Surf. Coat. Technol.* **2020**, *392*, 125755.

(164) Cheng, K. Y.; Gopal, V.; McNallan, M.; Manivasagam, G.; Mathew, M. T. Enhanced tribocorrosion resistance of hard ceramic coated Ti-6Al-4V alloy for hip implant application: in-vitro simulation study. *ACS Biomater. Sci. Eng.* **2019**, *5*, 4817−4824.

(165) Goldberg, J. R.; Gilbert, J. L. The electrochemical and mechanical behavior of passivated and TiN/AlN-coated CoCrMo and Ti6Al4V alloys. *Biomaterials* **2004**, *25*, 851−864.

(166) Nakagawa, M.; Matsuya, S.; Shiraishi, T.; Ohta, M. Effect of fluoride concentration and pH on corrosion behavior of titanium for dental use. *J. Dent. Res.* **1999**, *78*, 1568−1572.

(167) Nagarajan, S.; Rajendran, N. Surface characterisation and electrochemical behaviour of porous titanium dioxide coated 316L stainless steel for orthopaedic applications. *Appl. Surf. Sci.* **2009**, *255*, 3927−3932.

(168) Starikov, V. V.; Starikova, S. L.; Mamalis, A. G.; Lavrynenko, S. N.; Ramsden, J. J. The application of niobium and tantalum oxides for implant surface passivation. *J. Biol. Phys. Chem.* **2007**, *7* (4), 141−145.

(169) Sowa, M.; Kazek-Kesik, A.; Krzakała, A.; Socha, R. P.; Dercz, G.; Michalska, J.; Simka, W. Modification of niobium surfaces using plasma electrolytic oxidation in silicate solutions. *J. Solid State Electrochem.* **2014**, *18*, 3129−3142.

(170) Souza, J. C.; Henriques, M.; Oliveira, R.; Teughels, W.; Celis, J. P.; Rocha, L. A. Do oral biofilms influence the wear and corrosion behavior of titanium? *Biofouling* **2010**, *26*, 471−478.

(171) Souza, J. C.; Barbosa, S. L.; Ariza, E. A.; Henriques, M.; Teughels, W.; Ponthiaux, P.; Celis, J. P.; Rocha, L. A. How do titanium and Ti6Al4V corrode in fluoridated medium as found in the oral cavity? An in vitro study. *Mater. Sci. Eng., C* **2015**, *47*, 384−393.

(172) Ramel, C. F.; Lüssi, A.; Özcan, M.; Jung, R. E.; Hämmerle, C. H.; Thoma, D. S. Surface roughness of dental implants and treatment time using six different implantoplasty procedures. *Clin. Oral Implants Res.* **2016**, *27*, 776−781.

(173) Lin, T. H.; Tamaki, Y.; Pajarinen, J.; Waters, H. A.; Woo, D. K.; Yao, Z.; Goodman, S. B. Chronic inflammation in biomaterial-induced periprosthetic osteolysis: NF-κB as a therapeutic target. *Acta Biomater.* **2014**, *10*, 1−10.

(174) Kuwabara, T.; Ishikawa, F.; Kondo, M.; Kakiuchi, T. The role of IL-17 and related cytokines in inflammatory autoimmune diseases. *Mediators Inflamm.* **2017**, *2017*, 3908061.

(175) Weng, J.; Liu, Q.; Wolke, J. G.; Zhang, X.; de Groot, K. Formation and characteristics of the apatite layer on plasma-sprayed hydroxyapatite coatings in simulated body fluid. *Biomaterials* **1997**, *18*, 1027−1035.

(176) Kokubo, T.; Takadama, H. How useful is SBF in predicting in vivo bone bioactivity? *Biomaterials* **2006**, *27*, 2907−2915.

(177) Kokubo, T. Design of bioactive bone substitutes based on biomineralization process. *Mater. Sci. Eng., C* **2005**, *25*, 97−104.

(178) Kokubo, T.; Matsushita, T.; Takadama, H.; Kizuki, T. Development of bioactive materials based on surface chemistry. *J. Eur. Ceram. Soc.* **2009**, *29*, 1267−1274.

(179) Singh, G.; Singh, H.; Sidhu, B. S. Corrosion behavior of plasma sprayed hydroxyapatite and hydroxyapatite-silicon oxide coatings on AISI 304 for biomedical application. *Appl. Surf. Sci.* **2013**, *284*, 811−818.

(180) Ponsonnet, L.; Reybier, K.; Jaffrezic, N.; Comte, V.; Lagneau, C.; Lissac, M.; Martelet, C. Relationship between surface properties (roughness, wettability) of titanium and titanium alloys and cell behaviour. *Mater. Sci. Eng., C* **2003**, *23*, 551−560.

(181) Harvey, A. G.; Hill, E. W.; Bayat, A. Designing implant surface topography for improved biocompatibility. *Expert Rev. Med. Devices* **2013**, *10*, 257−267.

(182) Xie, W.; Wang, J.; Berndt, C. C. Ethylene methacrylic acid (EMAA) single splat morphology. *Coatings* **2013**, *3*, 82−97.

(183) Jung, U. W.; Hwang, J. W.; Choi, D. Y.; Hu, K. S.; Kwon, M. K.; Choi, S. H.; Kim, H. J. Surface characteristics of a novel hydroxyapatite-coated dental implant. *J. Periodontal Implant Sci.* **2012**, *42*, 59−63.

(184) Shekaran, A.; García, A. J. Extracellular matrix-mimetic adhesive biomaterials for bone repair. *J. Biomed. Mater. Res., Part A* **2011**, *96*, 261−272.

(185) Chai, F.; Ochsenbein, A.; Traisnel, M.; Busch, R.; Breme, J.; Hildebrand, H. F. Improving endothelial cell adhesion and proliferation on titanium by sol-gel derived oxide coating. *J. Biomed. Mater. Res., Part A* **2009**, *92A*, 754−765.

(186) Rohanová, D.; Boccaccini, A. R.; Horkavcová, D.; Bozdechová, P.; Bezdička, P.; Castorálová, M. Is non-buffered DMEM solution a suitable medium for in vitro bioactivity tests? *J. Mater. Chem. B* **2014**, *2*, 5068−5076.

(187) Shokouhinejad, N.; Nekoofar, M. H.; Razmi, H.; Sajadi, S.; Davies, T. E.; Saghiri, M. A.; Gorjestani, H.; Dummer, P. M. Bioactivity of EndoSequence root repair material and bioaggregate. *Int. Endod. J.* **2012**, *45*, 1127−1134.

(188) Vitorino, R.; Lobo, M. J.; Ferrer-Correira, A. J.; Dubin, J. R.; Tomer, K. B.; Domingues, P. M.; Amado, F. M. Identification of human whole saliva protein components using proteomics. *Proteomics* **2004**, *4*, 1109−1115.

(189) Tamaki, N.; Tada, T.; Morita, M.; Watanabe, T. Comparison of inhibitory activity on calcium phosphate precipitation by acidic proline-rich proteins, statherin, and histatin-1. *Calcif. Tissue Int.* **2002**, *71*, 59.

(190) Eanes, E.; Gillessen, I.; Posner, A. Intermediate states in the precipitation of hydroxyapatite. *Nature* **1965**, *208*, 365−367.

(191) Katta, P. P.; Nalliyan, R. Corrosion resistance with self-healing behavior and biocompatibility of Ce incorporated niobium oxide coated 316L SS for orthopedic applications. *Surf. Coat. Technol.* **2019**, *375*, 715−726.

(192) Pradeep PremKumar, K.; Duraipandy, N.; Manikantan Syamala, K.; Rajendran, N. Antibacterial effects, biocompatibility and electrochemical behavior of zinc incorporated niobium oxide coating on 316L SS for biomedical applications. *Appl. Surf. Sci.* **2018**, *427*, 1166−1181.

(193) Sharkeev, Y.; Komarova, E.; Sedelnikova, M.; Sun, Z. M.; Zhu, Q. F.; Zhang, J.; Tolkacheva, T.; Uvarkin, P. Structure and properties of micro-arc calcium phosphate coatings on pure titanium and Ti-40Nb alloy. *Trans. Nonferrous Met. Soc. China* **2017**, *27*, 125−133.

(194) Enayati, M.; Fathi, M.; Zomorodian, A. Characterisation and corrosion properties of novel hydroxyapatite niobium plasma sprayed coating. *Surf. Eng.* **2009**, *25*, 338−342.

(195) Jacobs, A.; Renaudin, G.; Forestier, C.; Nedelec, J.-M.; Descamps, S. Biological properties of copper-doped biomaterials for orthopedic applications: A review of antibacterial, angiogenic and osteogenic aspects. *Acta Biomater.* **2020**, *117*, 21−39.

(196) Chellan, P.; Sadler, P. J. The elements of life and medicines. *Philos. Trans. Royal Soc.* **2015**, *373*, 20140182.

(197) Lowe, N. M.; Fraser, W. D.; Jackson, M. J. Is there a potential therapeutic value of copper and zinc for osteoporosis? *Proc. Nutr. Soc.* **2002**, *61*, 181−185.

(198) Rojas, P.; Rodil, S. Corrosion behaviour of amorphous niobium oxide coatings. *Int. J. Electrochem. Sci.* **2012**, *7*, 1443−1458.

(199) Arsova, I.; Prusi, A.; Grčev, T.; Arsov, L. Electrochemical characterization of the passive films formed on niobium surfaces in H_2SO_4 solutions. *J. Serbian Chem.* **2006**, *71*, 177−187.

(200) Gagnon, J.; Fromm, K. M. Toxicity and protective effects of cerium oxide nanoparticles (nanoceria) depending on their preparation method, particle size, cell type, and exposure route. *Eur. J. Inorg. Chem.* **2015**, *2015*, 4510−4517.

(201) Zhou, G.; Gu, G.; Li, Y.; Zhang, Q.; Wang, W.; Wang, S.; Zhang, J. Effects of cerium oxide nanoparticles on the proliferation, differentiation, and mineralization function of primary osteoblasts in vitro. *Biol. Trace Elem. Res.* **2013**, *153*, 411−418.

(202) Niu, J.; Wang, K.; Kolattukudy, P. E. Cerium oxide nanoparticles inhibits oxidative stress and nuclear factor-κB activation in H9c2 cardiomyocytes exposed to cigarette smoke extract. *J. Pharmacol. Exp. Ther.* **2011**, *338*, 53−61.

(203) Korsvik, C.; Patil, S.; Seal, S.; Self, W. T. Superoxide dismutase mimetic properties exhibited by vacancy engineered ceria nanoparticles. *Chem. Commun.* **2007**, *2007*, 1056−1058.

(204) Hu, H.; Zhang, W.; Qiao, Y. Q.; Jiang, X. Y.; Liu, X.; Ding, C. Antibacterial activity and increased bone marrow stem cell functions of Zn-incorporated TiO_2 coatings on titanium. *Acta Biomater.* **2012**, *8*, 904−915.

(205) Applerot, G.; Lipovsky, A.; Dror, R.; Perkas, N.; Nitzan, Y.; Lubart, R.; Gedanken, A. Enhanced antibacterial activity of nanocrystalline ZnO due to increased ROS-mediated cell injury. *Adv. Funct. Mater.* **2009**, *19*, 842−852.

(206) Rai, M.; Kon, K.; Gade, A.; Ingle, A.; Nagaonkar, D.; Paralikar, P.; da Silva, S. S. Antibiotic Resistance: Can Nanoparticles Tackle the Problem? In *Antibiotic Resistance*; Academic Press, 2016; pp 121−143, DOI: 10.1016/B978-0-12-803642-6.00006-X.

(207) Devrim, B.; Bozkır, A. Nanocarriers and Their Potential Application as Antimicrobial Drug Delivery. In *Nanostructures for Antimicrobial Therapy*; Elsevier, 2017; pp 169−202.

(208) Grigore, M. E.; Biscu, E. R.; Holban, A. M.; Gestal, M. C.; Grumezescu, A. M. Methods of synthesis, properties and biomedical applications of CuO nanoparticles. *Pharmaceuticals* **2016**, *9*, 75.

(209) Perreault, F.; Melegari, S. P.; da Costa, C. H.; de Oliveira Franco Rossetto, A. L.; Popovic, R.; Matias, W. G. Genotoxic effects of copper oxide nanoparticles in Neuro 2A cell cultures. *Sci. Total Environ.* **2012**, *441*, 117−124.

(210) Baek, Y. W.; An, Y. J. Microbial toxicity of metal oxide nanoparticles (CuO, NiO, ZnO, and Sb_2O_3) to Escherichia coli, Bacillus subtilis, and Streptococcus aureus. *Sci. Total Environ.* **2011**, *409*, 1603−1608.

(211) Ruiz, P.; Katsumiti, A.; Nieto, J. A.; Bori, J.; Jimeno-Romero, A.; Reip, P.; Arostegui, I.; Orbea, A.; Cajaraville, M. P. Short-term effects on antioxidant enzymes and long-term genotoxic and carcinogenic potential of CuO nanoparticles compared to bulk CuO and ionic copper in mussels Mytilus galloprovincialis. *Mar. Environ. Res.* **2015**, *111*, 107−120.

(212) Sikka, M. P.; Midha, V. K. The Role of Biopolymers and Biodegradable Polymeric Dressings in Managing Chronic Wounds. In *Advanced Textiles for Wound Care*; Elsevier, 2019; pp 463−488.

(213) Gera, S.; Kankuri, E.; Kogermann, K. Antimicrobial peptides-Unleashing their therapeutic potential using nanotechnology. *Pharmacol. Ther.* **2021**, 107990.

(214) Schafhauser, B. H.; Kristofco, L. A.; de Oliveira, C. M.; Brooks, B. W. Global review and analysis of erythromycin in the environment: occurrence, bioaccumulation and antibiotic resistance hazards. *Environ. Pollut.* **2018**, *238*, 440−451.

(215) Munckhof, W. J.; Borlace, G.; Turnidge, J. D. Postantibiotic suppression of growth of erythromycin A-susceptible and-resistant gram-positive bacteria by the ketolides telithromycin (HMR 3647) and HMR 3004. *Antimicrob. Agents Chemother.* **2000**, *44*, 1749−1753.

(216) Pokkunuri, I.; Champney, W. S. Characteristics of a 50S ribosomal subunit precursor particle as a substrate for ermE methyltransferase activity and erythromycin binding in Staphylococcus aureus. *RNA boil.* **2007**, *4*, 147−153.